The compressibility of minimal lattice knots

J. Stat. Mech. (2012) P05003

(http://iopscience.iop.org/1742-5468/2012/05/P05003)

Journal of Statistical Mechanics: Theory and Experiment
An IOP and SISSA journal

The compressibility of minimal lattice knots

E J Janse van Rensburg[1] **and A Rechnitzer**[2]

[1] Department of Mathematics and Statistics, York University, Toronto, ON M3J 1P3, Canada
[2] Department of Mathematics, The University of British Columbia, Vancouver V6T 1Z2, BC, Canada
E-mail: rensburg@yorku.ca and andrewr@math.ubc.ca

Received 16 March 2012
Accepted 7 April 2012
Published 3 May 2012

Online at stacks.iop.org/JSTAT/2012/P05003
doi:10.1088/1742-5468/2012/05/P05003

Abstract. The (isothermic) compressibility of lattice knots can be examined as a model of the effects of topology and geometry on the compressibility of ring polymers. In this paper, the compressibilities of minimal length lattice knots in the simple cubic, face centered cubic and body centered cubic lattices are determined. Our results show that the compressibility is generally not monotonic, but in some cases increases with pressure. Differences in the compressibility for different knot types show that the topology is a factor determining the compressibility of a lattice knot, and differences between the three lattices show that the compressibility is also a function of the geometry.

Keywords: loop models and polymers, classical Monte Carlo simulations, mechanical properties (DNA, RNA, membranes, bio-polymers) (theory), polymer elasticity

ArXiv ePrint: 1203.3212

1742-5468/12/P05003+31$33.00

Contents

1. Introduction

The compressibility of polymer colloids and melts, and also of biopolymers, is an important physical property which affects the rheology and other physical properties [20, 28]. The compressibility of linear polymers is monotonic non-increasing with pressure (see, for example, figure I in [20] or figures 15 and 16 in [28]), and typically approaches zero with increasing pressure.

In this paper, we will examine a model of the compressibility of tightly knotted ring polymers, where entanglements become an important factor in addition to the geometry in determining the thermodynamic properties of the polymer. We do so by examining the compressibility of a lattice model of a knotted ring polymer.

Lattice polygons were introduced as a model of polymer entropy in ring polymers [9, 4]. In three dimensions a ring polymer may be knotted, and it is known that the topological properties of ring polymers have an important effect on their entropy [8, 5]. Lattice knots are now a standard model for the polymer entropy problem in knotted ring polymers [22, 26, 10] and these objects have been the subject of numerous studies over the last two decades [19, 12, 27, 21, 11, 18, 25, 23]. One of the advantages in models of lattice

J. Stat. Mech. (2012) P05003

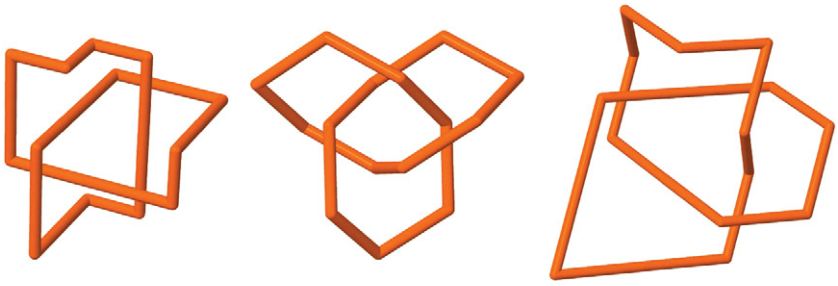

Figure 1. Examples of minimal length lattice trefoils (knot type 3_1^+ in the standard knot tables [3]) in three-dimensional cubic lattices. These are embeddings in the simple cubic lattice (left), the face centered cubic lattice (middle), and the body centered cubic lattice (right).

knots is that they are effective numerical models for simulating the effects of topological constraints (knotting) on the properties of ring polymers, and although one may not obtain direct quantitative results for real ring polymers, qualitative results may be examined to gain insight into the physical properties of ring polymers generally.

The entropy of a ring polymer depends on its length (number of monomers) and on knots along the backbone of the polymer. Ring polymers which are too short cannot accommodate a knot, and one expects that for each knot type there will be a minimal length which will allow the knot to be realized in the polymer. This situation is modeled by minimal length lattice knots [6, 7], which are idealized models of knotted ring polymers of minimal length (or equivalently, maximal thickness).

Examples of minimal length lattice knots in the simple cubic, face centered cubic, and body centered cubic lattices are illustrated in figure 1.

Minimal length embeddings of lattice knots have residual conformational entropy (in addition to entropic contributions from translational and rotational degrees of freedom). For example, it is known that there are 75 distinct symmetry classes of right handed lattice trefoil knots, which expand to 1664 distinct polygons when one accounts for rotational degrees of freedom as well [25].

The residual conformational degrees of freedom of minimal length lattice knots may seem a surprising feature of these models, and are known to be very dependent on the particular lattice [16]. However, minimal length ring polymers will similarly have some residual conformational degrees of freedom, even if tightly knotted. This would be because the discrete values of angles between adjacent bonds joining the monomers will admit different local geometric arrangements in the embedding of the polymer in free space. These arrangements will contribute to the entropy of the polymer, which is generally a function of the local geometry of the bonding (bonding angles, bond lengths). It will also be a function of the knot type if the polymer is knotted. The overall topology of the knotted polymer will constrain the molecule even locally to entangle in particular ways to complete the knot, in particular when it has minimal length. This will determine in some measure the entropy of the polymer.

In other words, while the entropic properties of minimal length lattice polygons will not produce quantitative results of real minimal length knotted ring polymers due to essential differences between the geometry of the lattice and polymers in three space,

J. Stat. Mech. (2012) P05003

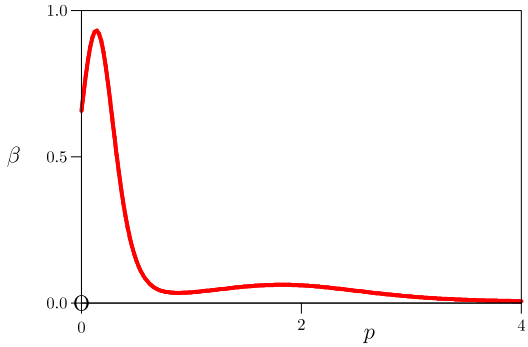

Figure 2. Compressibility of the minimal lattice knot of type 3_1^+ in the SC lattice.

lattice knots are nevertheless a useful model to examine the qualitative nature of the interplay between topology and entropy in ring polymers.

In this paper we examine the (isothermal) compressibility of lattice knots as a model of the effects of pressure and topology on tightly knotted polymers. The compressibility will be defined by assuming the lattice knot to be in a bath of solvent molecules which are excluded from a volume about the lattice knot. The response of the lattice knot to increasing pressure in the solvent will be determined, and its compressibility thus determined.

Our numerical approach will be to determine the compressibility from exact numerical data on minimal length lattice knots obtained by using the GAS algorithm for lattice knots [14, 15]. An excluded volume containing the lattice knot will be defined, and changes in its mean size due to an externally applied pressure will be used to calculate the compressibility of the lattice knot as it is compressed in this volume.

Our approach defines an internal space close to the polygon which excludes solvent molecules, and increasing the ambient pressure will then compress the containing volume and the lattice knot inside it. We shall define two different volumes for this purpose: the first will be the smallest rectangular box containing the polygon, and the second will be a more close-fitting envelope which will be defined using slices defined by the two-dimensional convex hulls of intersections of lattice knots with lattice planes. The second volume is not necessarily convex, and will in many cases be smaller than the convex hull of the polygon, which is much harder to determine. We shall repeat these calculations for the three cubic lattices, namely the simple cubic lattice (SC), the face centered cubic lattice (FCC) and the body centered cubic lattice (BCC).

In virtually all cases the lattice knots will be found to be compressible in general. Moreover, the compressibility will be found to have complicated and unexpected dependence on the applied pressure in some knot types, even exhibiting increasing compressibility with increasing pressure for some ranges of the applied pressure. For example, the compressibility β of a lattice trefoil in a pressurized rectangular box in the simple cubic lattice is shown in figure 2. β increases with small pressures to a peak, it then declines, and reaches a local maximum at intermediate pressures before it decreases to zero with large pressures. This unusual shape for the (p, β) curve shows that lattice trefoils may become relatively softer with increasing pressure in some pressure ranges—this kind of result would be dependent on both the lattice geometry and the topology of

J. Stat. Mech. (2012) P05003

the polygon, and so would not necessarily give a qualitative indication of the nature of real compressed ring polymers. However, the result suggests that this kind of behavior is possible, as it is observed to some extent in all three of the lattices we considered. Generally, however, different curves will be obtained for β in the other lattices.

We have organized our paper as follows. In section 2 our methods and definitions are presented and explained. In section 3 we present results and discuss our findings. We conclude the paper in section 4.

2. The compressibility of minimal length lattice knots

The SC lattice will be realized as $\mathbb{Z}^3$ with basis $\{(1,0,0),(0,1,0),(0,0,1)\}$ and edges of length 1. The FCC lattice has basis $\{(\pm1,\pm1,0),(\pm1,0,\pm1),(0,\pm1,\pm1)\}$ for all possible choices of the signs, and edges between adjacent vertices of length $\sqrt{2}$, while the BCC will have basis $\{(\pm1,\pm1,\pm1)\}$ for all possible choices of the signs, and edges of length $\sqrt{3}$.

Polygons in the SC, FCC and BCC lattices are sequences of vertices and edges $\{v_0,e_1,v_1,e_2,v_2,\ldots,v_{n-1},e_n,v_n\}$ where $v_0=v_n$ and all the vertices v_i are distinct. Then the end-vertices of edges e_i are v_{i-1} and v_i. The *length* of a polygon ω is the number of edges it contains, and the *chemical length* will be the length times the length of edges: for example, if a polygon has length n, then its chemical length in the SC lattice is n, in the FCC lattice is $n\sqrt{2}$ and in the BCC lattice is $n\sqrt{3}$, since edges have lengths 1, $\sqrt{2}$ and $\sqrt{3}$ in the SC, FCC and BCC lattices respectively. In other words, the chemical length coincides with the geometric length of the polygons.

Polygons will be considered to be identical if one is a translation of another. Define $\mathcal{P}_K$ to be the set of minimal length lattice polygons of knot type K and length n_K. The cardinality of $\mathcal{P}_K$ is the number of polygons of knot type K and minimal length, and this is denoted by $p_L(K)=|\mathcal{P}_K|$ in the lattice L. For example, $p_{\mathrm{SC}}(0_1)=3$, $p_{\mathrm{FCC}}(0_1)=8$ while $p_{\mathrm{BCC}}(0_1)=12$. The minimal length of the unknot in the SC lattice is 4, while in the FCC lattice it is 3 and in the BCC lattice it is 4.

In order to determine the compressibility of lattice knots, it is necessary to define the volume they occupy. An upper bound on the excluded volume of a lattice knot is the minimal volume rectangular box with sides parallel to the X-, Y- and Z-axes containing it. A lower bound can be obtained by noting that a particular lattice knot ω should occupy at least the sites along its length, and also the intersection of the minimal rectangular box containing it with the union of the Wigner–Seitz cells along its length. This lower bound is perhaps too small, as the interstitial space surrounded by vertices of the lattice knot should also be part of the excluded volume. Hence, we choose to require the excluded volume of a lattice knot to be a convex region containing the knot.

In the first instance, the smallest rectangular box in the lattice containing the lattice knot was taken as an excluded volume V_{b} about the knot. A second, smaller excluded volume V_{e} was defined by slicing the lattice knot with lattice planes, computing convex hulls in these planes, and then gluing them in slabs together to find a more tightly fitting volume about the lattice knot. We call this volume the *average excluded volume* V_{e} of the lattice knot. A more careful definition is given below. In both cases we assume that solvent molecules pressurizing the lattice knot are excluded from the excluded volume V_{b} and V_{e}, and increases in pressure in the solvent will pressurize the knot by exerting a pressure on the convex boundary of the volume about the lattice polygon.

J. Stat. Mech. (2012) P05003

Once the volumes containing lattice knots have been defined, they can be pressurized in these volumes and their compressibility determined. In this study we focus on the compressibility of lattice knots by using the minimal rectangular box and average excluded volume.

2.1. The rectangular box volume of lattice polygons

The volume of the smallest rectangular box with sides normal to the lattice axes containing a lattice knot is its *box volume* $V_{\rm b}$. This volume is a large overestimate of the volume occupied by the polygon, since it is likely to include large spaces near the eight corners of the box. Observe that if $V_{\rm C}$ is the volume of the convex hull of a polygon, then in general $V_{\rm C} \leq V_{\rm b}$, although both volumes are minimal convex shapes containing the polygon.

Define $p_L(v;K)$ to be the number of minimal length lattice polygons in a lattice L, of knot type K, minimal box volume v. Then $\sum_v p_L(v;k) = p_L(K)$ is the total number of minimal length lattice polygons of knot type K.

One may check that $p_{\rm SC}(0;0_1) = 3$ but $p_{\rm FCC}(1;0_1) = 8$. However $p_{\rm BCC}(8;0_1) = 6$ and $p_{\rm BCC}(4;0_1) = 6$, since there are two classes of minimal length unknotted polygons in the BCC lattice, one class of six elements in a minimal rectangular box of dimensions $2 \times 2 \times 2$, and a second class of six elements in a minimal rectangular box of dimensions $2 \times 2 \times 1$.

2.2. The average excluded volume of lattice polygons

Let ω be a lattice knot and P_z be a lattice plane normal to the Z-axis. For some choices of P_z the intersection $\omega \cap P_z = Q_\omega$ is not empty but contains a subset of vertices from ω. Let C_z be the convex hull of the points in Q_ω, then C_z is a (geometric) two-dimensional polygon in the plane P_z.

Suppose that the (integer) values of z giving a non-empty intersection Q_ω are $\{z_0, z_1, \ldots, z_m\}$ with $z_{i-1} + 1 = z_i$ for $i = 1, 2, \ldots, m$.

Define the slab $S_z = C_z[z - 1/2, z + 1/2]$ for each $z = z_i$ with $i = 1, 2, \ldots, m-1$. In addition, define $S_{z_0} = C_{z_0}[z_0, z_0 + 1/2]$ and $S_{z_m} = C_{z_m}[z_m - 1/2, z_m]$.

Define the volume V_z about ω by taking the union of these slabs:

$$V_z = \bigcup_{i=0}^{m} S_{z_i}.$$

Observe that the vertices of ω are contained in V_z, but that some edge may in fact be partially exposed. Since excluded volume effects in lattice polygons are defined in terms of vertices avoiding one another, we still consider V_z to constitute a volume containing ω, but it fits very tightly about the polygon in general.

The volumes V_x and V_y can be defined in this way by cutting ω by lattice planes normal to the X-axis or Y-axis instead. Taking the average gives the *average excluded volume* $V_{\rm e}$ of ω:

$$V_{\rm e} = (V_x + V_y + V_z)/3.$$

It is observed that $V_{\rm e} \leq V_{\rm b}$. One may also show that $V_{\rm e} = 0$ for minimal length unknotted polygons in the SC, FCC and BCC lattices.

J. Stat. Mech. (2012) P05003

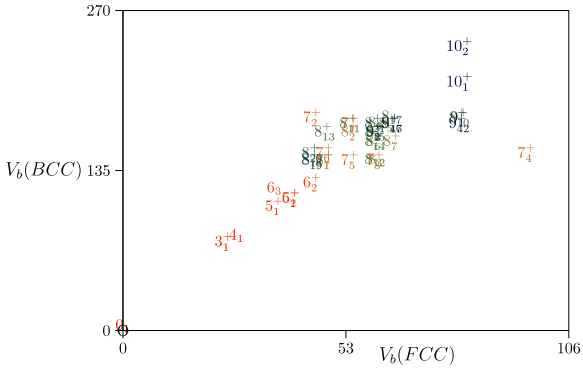

Figure 3. A scatter plot of the minimum rectangular box volumes V_b of knot types in the FCC and BCC. The points are contained in a narrow wedge, and the volumes are strongly correlated.

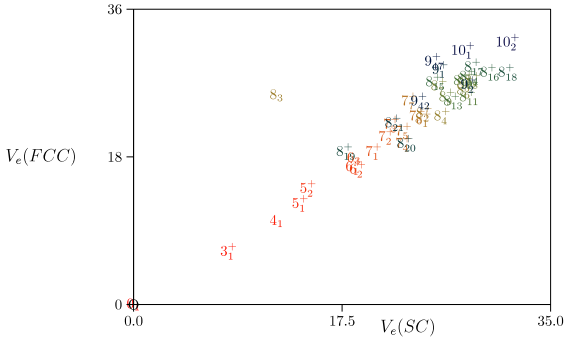

Figure 4. A scatter plot of the minimum average excluded volumes V_e of knot types in the SC and FCC. The points, with the exception of 8_3, are contained in a narrow wedge, and the volumes are strongly correlated.

The values of V_e in the three lattices are strongly correlated across knot types. For example, in figure 4 a scatter plot of V_e in the SC and FCC is illustrated. The minimal values of V_e in the FCC and BCC are similarly plotted in figure 5 showing a strong correlation between these minimal volumes in the FCC and BCC lattices.

The minimal values of V_b and V_e are strongly correlated for different knot types. For example, if the minimum value of V_b is relatively small for a knot type K, then so is the minimum value of V_e. In figure 6 the minimal values of $(V_\mathrm{b}, V_\mathrm{e})$ are illustrated in a scatter plot for the SC lattice.

2.3. The compressibility of minimal length lattice polygons

Consider a minimal lattice knot ω in a volume v_ω (which may be either the minimal box volume V_b, or the average excluded volume V_e). If the lattice knot is pressurized by an external pressure p, then its statistical mechanics properties will be described by its partition function, given by

$$\mathcal{Z}_L(K) = \sum_v p_L(v;K)\mathrm{e}^{-p\,v}$$

J. Stat. Mech. (2012) P05003

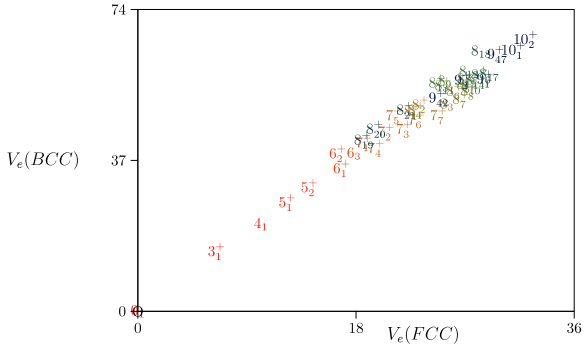

Figure 5. A scatter plot of the minimum average excluded volumes V_e of knot types in the FCC and BCC. The points are contained in a narrow wedge, and the volumes are strongly correlated.

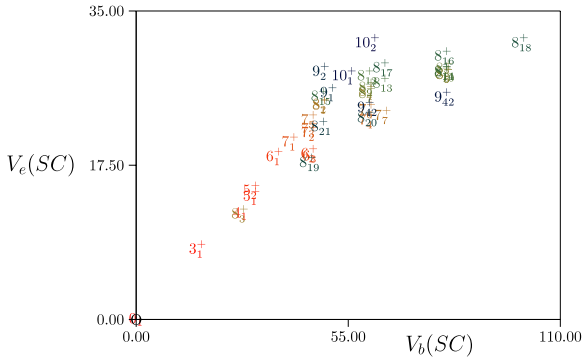

Figure 6. A scatter plot of $\min V_e(K)$ and $\min V_b(K)$ in the SC lattice for knot types K as indicated. The points are contained in a narrow wedge, and the volumes are strongly correlated.

where the pressure and volume are in lattice units, and the Boltzmann factor is put equal to unity.

For example, the partition functions of minimal unknotted polygons with volumes V_b are given by

$$\mathcal{Z}_{SC}(0_1) = 3, \qquad \mathcal{Z}_{FCC}(0_1) = 8e^{-p}, \qquad \mathcal{Z}_{BCC}(0_1) = 6e^{-8p} + 6e^{-4p}.$$

If the volume V_e is used instead, then

$$\mathcal{Z}_{SC}(0_1) = 3, \qquad \mathcal{Z}_{FCC}(0_1) = 8, \qquad \mathcal{Z}_{BCC}(0_1) = 12.$$

The free energy of these models can be computed in the usual way: $\mathcal{F}_L(K) = -\log \mathcal{Z}_L(K)$. For example, the free energy of minimal length unknotted polygons in the BCC lattice in the rectangular box volume V_b is given by

$$\mathcal{F}_{BCC}(0_1) = -\log(6e^{-8p} + 6e^{-4p}). \tag{1}$$

This is explicitly dependent on p, and shows that pressurizing minimal length unknotted BCC lattice polygons will lead to a response by adjusting the average equilibrium volume occupied by the polygon.

J. Stat. Mech. (2012) P05003

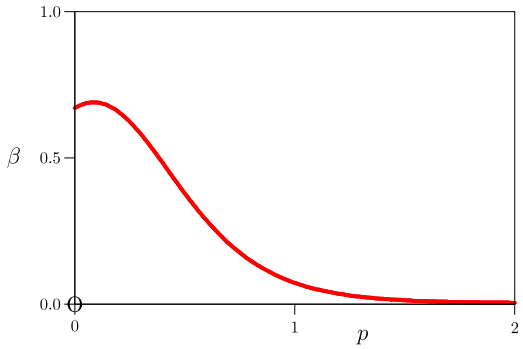

Figure 7. Compressibility of the BCC minimal lattice knot of type 0_1 in a rectangular box of volume V_b. Observe the global maximum at $p = 0.086\,64\cdots$ where $\beta = 0.686\,29\cdots$. If $p = 0$, then $\beta = 2/3$.

In the other cases the polygon will not respond to increasing pressure, and it is incompressible.

The average (equilibrium) volume occupied by a minimal length lattice knot at pressure p is obtained by

$$\langle V\rangle_L = \frac{\partial \mathcal{F}_L(K)}{\partial p}.$$

The compressibility of the body is defined by

$$\beta = -\frac{\partial \log\langle V\rangle_L}{\partial p},$$

and this definition shows that β is the fractional change in expected volume due to an increment in pressure. β is generally a function of temperature and pressure, and, since temperature is fixed in this model, this is in particular the isothermal compressibility.

The average occupied rectangular box volume and compressibility of the minimal length unknot in the BCC lattice are as follows.

$$\langle V_b\rangle_{BCC} = \frac{4(1+2e^{-4p})}{1+e^{-4p}}.$$

When $p = 0$ this gives $\langle V_b\rangle_{BCC} = 6$ and if $p \to \infty$ then $\langle V_b\rangle_{BCC} = 4$. The compressibility can be computed directly:

$$\beta_{BCC}(0_1) = \frac{4e^{-4p}}{(1+e^{-4p})(1+2e^{-4p})}.$$

For the minimal length unknot in the other lattices, and also for the choice of V_e in all cases, the compressibility of the unknot is zero (that is, it is not compressible). The compressibility of the unknot in the BCC lattice with volume V_b is plotted in figure 7.

The minimum rectangular box volume containing a lattice knot K is its *minimal rectangular box volume* (in the case of V_b), or its *minimal average excluded volume* (in the case of V_e). If a lattice knot is allowed to expand from its minimal volume to its equilibrium volume at zero pressure, there is a change in its free energy. The maximum amount of useful work that can be extracted from this expansion, if the process is reversible, is given by the difference in free energies between the state at $p = 0$ (when the lattice knot is in

an equilibrium state at zero pressure) and the state were the lattice knot is confined to its minimal volume.

Since the free energy of the unknot is independent of the pressure for the volume V_e, no useful work can be performed by a compressed unknot in any of the lattices. With the choice of volume V_b, the one exception is in the BCC lattice where $\mathcal{F}_{BCC}(0_1)$ is given by equation (1). Direct calculation shows that the maximum amount of work that can be performed by letting this polygon expand reversibly from its compressed state is $\mathcal{W}_{0_1} = \log 12 - \log 6 = \log 2$.

3. Compressibilities of lattice knots: numerical results

3.1. GAS sampling of lattice knots

In this study we have sampled minimal length lattice polygons by implementing the GAS algorithm [14, 15]. The algorithm is implemented using a set of local elementary transitions (called 'atmospheric moves' [13]) to sample along sequences of polygon conformations. The algorithm is a generalization of the Rosenbluth algorithm [24], and is an approximate enumeration algorithm.

The GAS algorithm can be implemented in the SC lattice on polygons of given knot type K using the BFACF elementary moves [1, 2] to implement the atmospheric moves [15, 16]. This implementation is irreducible on classes of polygons of fixed knot type [17].

Atmospheric moves in the FCC and BCC lattices were defined in [16], and implemented using the GAS algorithm. As in the SC lattice, these atmospheric moves are irreducible on polygon classes of fixed knot type.

The implementation is described in detail in [15, 16]. Polygons of fixed knot type were sampled along sequences, tracking their lengths and metric properties. Minimal length polygons were detected, classified by symmetry class, stored by hashing and written to disk for later analysis.

The GAS algorithm was implemented efficiently using hash coding which allowed elementary moves to be executed in $O(1)$ CPU time, independent of length. This efficiency allowed us to perform billions of iterations on knotted polygons in reasonable real time on desktop linux workstations. Simulations were performed by sampling up to 500 GAS sequences, each of length 10^7, to search and collect minimal length polygons. In most cases the minimal length polygons were detected fairly quickly, although some knot types proved a little harder and required more CPU time.

Data on minimal knots were collated and analyzed separately. Minimal volumes V_b and V_e were computed for the symmetry classes of the polygons and collected into expressions for the partition functions, from which free energies and compressibilities were computed.

3.2. Compressibilities of minimal length lattice knots in the SC lattice

The partition functions of minimal length lattice knots with volumes given by V_b and up to seven crossings are given in table 1. The partition functions of minimal lattice knots with volumes V_e (average excluded volumes) are listed in table 2 up to five crossing knots. These expressions are typically far more complicated than those in table 1. By examining

J. Stat. Mech. (2012) P05003

Table 1. Partition functions: minimal SC lattice knots in a pressurized rectangular box.

Knot	$\mathcal{Z}_{\mathrm{SC}}(p)$
0_1	3
3_1^+	$1220\mathrm{e}^{-27p} + 432\mathrm{e}^{-18p} + 12\mathrm{e}^{-16p}$
4_1	$2784\mathrm{e}^{-36p} + 864\mathrm{e}^{-27p}$
5_1^+	$432\mathrm{e}^{-48p} + 624\mathrm{e}^{-36p} + 2160\mathrm{e}^{-32p} + 120\mathrm{e}^{-30p}$
5_2^+	$40\,536\mathrm{e}^{-48p} + 4200\mathrm{e}^{-45p} + 10\,560\mathrm{e}^{-36p} + 2160\mathrm{e}^{-30p}$
6_1^+	$2640\mathrm{e}^{-48p} + 216\mathrm{e}^{-45p} + 216\mathrm{e}^{-36p}$
6_2^+	$7560\mathrm{e}^{-64p} + 5256\mathrm{e}^{-60p} + 3504\mathrm{e}^{-48p} + 96\mathrm{e}^{-45p}$
6_3	$2208\mathrm{e}^{-64p} + 912\mathrm{e}^{-48p} + 432\mathrm{e}^{-45p}$
7_1^+	$288\mathrm{e}^{-80p}+252\mathrm{e}^{-64p}+11\,808\mathrm{e}^{-60p}+300\mathrm{e}^{-54p}+468\mathrm{e}^{-48p}+264\mathrm{e}^{-45p}+3600\mathrm{e}^{-40p}$
7_2^+	$22404\mathrm{e}^{-80p} + 2880\mathrm{e}^{-75p} + 13\,032\mathrm{e}^{-64p} + 85\,008\mathrm{e}^{-60p} + 11\,712\mathrm{e}^{-54p} + 22\,512\mathrm{e}^{-48p} + 10\,632\mathrm{e}^{-45p}$
7_3^+	$240\mathrm{e}^{-45p}$
7_4^+	$24\mathrm{e}^{-64p} + 60\mathrm{e}^{-60p}$
7_5^+	$4392\mathrm{e}^{-64p} + 216\mathrm{e}^{-60p} + 96\mathrm{e}^{-48p} + 24\mathrm{e}^{-45p}$
7_6^+	$10\,368\mathrm{e}^{-80p} + 4728\mathrm{e}^{-64p} + 1920\mathrm{e}^{-60p}$
7_7^+	$168\mathrm{e}^{-80p} + 84\mathrm{e}^{-64p}$

the partition functions in tables 1 and 2 the compressibilities and other properties of the minimal length lattice knots can be determined exactly.

3.2.1. Compressibility of 3_1^+ in the SC lattice. The compressibility of the trefoil knot displayed in figure 2 was obtained by choosing the volume V_{b} in the SC lattice. The partition function in this case is given by

$$\mathcal{Z}_{\mathrm{SC}}(3_1^+) = 1220\mathrm{e}^{-27p} + 432\mathrm{e}^{-18p} + 12\mathrm{e}^{-16p}. \tag{2}$$

The expected volume of the lattice knot at pressure p is

$$\langle V_{\mathrm{b}} \rangle = \frac{3(2745\mathrm{e}^{-27p} + 648\mathrm{e}^{-18p} + 16\mathrm{e}^{-16p})}{305\mathrm{e}^{-27p} + 108\mathrm{e}^{-18p} + 3\mathrm{e}^{-16\,p}}$$

and the compressibility is explicitly given by

$$\beta = \frac{889\,380\mathrm{e}^{-45p} + 36\,905\mathrm{e}^{-43p} + 432\mathrm{e}^{-34p}}{(2745\mathrm{e}^{-27p} + 648\mathrm{e}^{-18p} + 16\mathrm{e}^{-16p})(305\mathrm{e}^{-27p} + 108\mathrm{e}^{-18p} + 3\mathrm{e}^{-16p})}.$$

Plotting this function for $p \in [0, 4]$ gives the curve in figure 2.

The compressibility of 3_1^+ is not monotonic with increasing p but first goes through a global maximum and then again later through a local maximum at higher pressure. Paradoxically, the lattice knot becomes 'softer' when compressed for some ranges of the pressure, in the sense that the fractional decrease in volume increases with p in some instances. This effect is likely due to the choice of V_{b} as an enclosing volume—as the pressure increases, the lattice knot starts to explore conformations which expand into the corners of the containing box more frequently, with the result that there is still space

J. Stat. Mech. (2012) P05003

Table 2. Partition functions: minimal SC lattice knots pressurized in their average excluded volumes.

Knot	$\mathcal{Z}_{\mathrm{SC}}(p)$
0_1	3
3_1^+	$84\mathrm{e}^{-32p/3} + 24\mathrm{e}^{-65p/6} + 300\mathrm{e}^{-10p} + 96\mathrm{e}^{-61p/6} + 240\mathrm{e}^{-59p/6} + 128\mathrm{e}^{-21p/2} + 48\mathrm{e}^{-28p/3} + 168\mathrm{e}^{-31p/3} + 48\mathrm{e}^{-19/2p} + 72\mathrm{e}^{-29p/3} + 12\mathrm{e}^{-11p} + 72\mathrm{e}^{-103p/12} + 192\mathrm{e}^{-53p/6} + 48\mathrm{e}^{-26p/3} + 24\mathrm{e}^{-35p/4} + 48\mathrm{e}^{-17/2p} + 24\mathrm{e}^{-25p/3} + 24\mathrm{e}^{-101p/12} + 12\mathrm{e}^{-8p}$
4_1	$48\mathrm{e}^{-155p/12} + 48\mathrm{e}^{-43p/3} + 192\mathrm{e}^{-79p/6} + 96\mathrm{e}^{-151p/12} + 96\mathrm{e}^{-25p/2} + 96\mathrm{e}^{-175p/12} + 96\mathrm{e}^{-38p/3} + 96\mathrm{e}^{-13p} + 192\mathrm{e}^{-173p/12} + 144\mathrm{e}^{-55p/4} + 192\mathrm{e}^{-77p/6} + 288\mathrm{e}^{-14p} + 48\mathrm{e}^{-59p/4} + 96\mathrm{e}^{-12p} + 48\mathrm{e}^{-41p/3} + 144\mathrm{e}^{-40p/3} + 96\mathrm{e}^{-53p/4} + 96\mathrm{e}^{-167p/12} + 432\mathrm{e}^{-83p/6} + 192\mathrm{e}^{-85p/6} + 48\mathrm{e}^{-157p/12} + 192\mathrm{e}^{-57p/4} + 240\mathrm{e}^{-161p/12} + 192\mathrm{e}^{-27p/2} + 240\mathrm{e}^{-163p/12}$
5_1^+	$96\mathrm{e}^{-29/2} + 48\mathrm{e}^{-173p/12} + 240\mathrm{e}^{-185p/12} + 264\mathrm{e}^{-91p/6} + 144\mathrm{e}^{-59p/4} + 72\mathrm{e}^{-187p/12} + 192\mathrm{e}^{-61p/4} + 264\mathrm{e}^{-181p/12} + 120\mathrm{e}^{-175p/12} + 120\mathrm{e}^{-43p/3} + 96\mathrm{e}^{-44p/3} + 288\mathrm{e}^{-89p/6} + 264\mathrm{e}^{-31p/2} + 204\mathrm{e}^{-15p} + 276\mathrm{e}^{-46p/3} + 144\mathrm{e}^{-179p/12} + 252\mathrm{e}^{-47p/3} + 168\mathrm{e}^{-95p/6} + 12\mathrm{e}^{-16p} + 24\mathrm{e}^{-14p} + 48\mathrm{e}^{-169p/12}$
5_2^+	$2496\mathrm{e}^{-109p/6} + 792\mathrm{e}^{-115p/6} + 72\mathrm{e}^{-47p/3} + 48\mathrm{e}^{-20p} + 48\mathrm{e}^{-179p/12} + 192\mathrm{e}^{-235p/12} + 912\mathrm{e}^{-229p/12} + 1320\mathrm{e}^{-71p/4} + 1536\mathrm{e}^{-227p/12} + 24\mathrm{e}^{-181p/12} + 504\mathrm{e}^{33p/2} + 720\mathrm{e}^{-77p/4} + 2232\mathrm{e}^{-35p/2} + 600\mathrm{e}^{-39p/2} + 1656\mathrm{e}^{-209p/12} + 1440\mathrm{e}^{-215p/12} + 72\mathrm{e}^{-61p/4} + 1584\mathrm{e}^{-113p/6} + 768\mathrm{e}^{-67p/4} + 120\mathrm{e}^{-46p/3} + 696\mathrm{e}^{-205p/12} + 264\mathrm{e}^{-187p/12} + 2088\mathrm{e}^{-53p/3} + 384\mathrm{e}^{-59p/3} + 1392\mathrm{e}^{-103p/6} + 192\mathrm{e}^{-119p/6} + 1152\mathrm{e}^{-17p} + 456\mathrm{e}^{-199p/12} + 408\mathrm{e}^{-49p/3} + 2184\mathrm{e}^{-56p/3} + 72\mathrm{e}^{-15p} + 360\mathrm{e}^{-63p/4} + 72\mathrm{e}^{-185p/12} + 504\mathrm{e}^{-65p/4} + 1608\mathrm{e}^{-52p/3} + 1224\mathrm{e}^{-211p/12} + 1728\mathrm{e}^{-221p/12} + 216\mathrm{e}^{-95p/6} + 3264\mathrm{e}^{-107p/6} + 2496\mathrm{e}^{-37p/2} + 384\mathrm{e}^{-197p/12} + 120\mathrm{e}^{-79p/4} + 1728\mathrm{e}^{-223p/12} + 1056\mathrm{e}^{-101p/6} + 2916\mathrm{e}^{-18p} + 168\mathrm{e}^{-191p/12} + 312\mathrm{e}^{-97p/6} + 1200\mathrm{e}^{-75p/4} + 1728\mathrm{e}^{-73p/4} + 24\mathrm{e}^{-59p/4} + 768\mathrm{e}^{-203p/12} + 336\mathrm{e}^{-193p/12} + 600\mathrm{e}^{-50p/3} + 2712\mathrm{e}^{-55p/3} + 24\mathrm{e}^{-121p/6} + 1128\mathrm{e}^{-58p/3} + 24\mathrm{e}^{-44p/3} + 276\mathrm{e}^{-16p} + 1224\mathrm{e}^{-69p/4} + 96\mathrm{e}^{-91p/6} + 120\mathrm{e}^{-31p/2} + 1200\mathrm{e}^{-217p/12} + 480\mathrm{e}^{-233p/12} + 936\mathrm{e}^{-19p}$

to expand into and compensate for the increasing pressure. The maxima in figure 2 can be determined numerically. The global maximum is located at $p = 0.135\,57\cdots$ where $\beta = 0.928\,45\cdots$. The local maximum is located at $p = 1.821\,15\cdots$ where $\beta = 0.058\,88\cdots$. The compressibility at zero pressure is $\beta = 0.653\,47\cdots$.

These results should be compared when the SC lattice knot of type 3_1^+ is instead considered but in the more tightly containing average excluded volume V_{e}. In this case the partition function is given by

$$\begin{aligned}\mathcal{Z}_{\mathrm{SC}}(3_1^+) = {} & 84\mathrm{e}^{-32p/3} + 24\mathrm{e}^{-65p/6} + 300\mathrm{e}^{-10p} + 96\mathrm{e}^{-61p/6} \\ & + 240\mathrm{e}^{-59p/6} + 128\mathrm{e}^{-21p/2} + 48\mathrm{e}^{-28p/3} + 168\mathrm{e}^{-31p/3} \\ & + 48\mathrm{e}^{-19/2p} + 72\mathrm{e}^{-29p/3} + 12\mathrm{e}^{-11p} + 72\mathrm{e}^{-103p/12} \\ & + 192\mathrm{e}^{-53p/6} + 48\mathrm{e}^{-26p/3} + 24\mathrm{e}^{-35p/4} + 48\mathrm{e}^{-17/2p} \\ & + 24\mathrm{e}^{-25p/3} + 24\mathrm{e}^{-101p/12} + 12\mathrm{e}^{-8p}. \end{aligned} \tag{3}$$

The compressibility can be determined in this model as above. It is plotted in figure 8. In this case one notes that the scale of the β-axis is an order of magnitude smaller than the

J. Stat. Mech. (2012) P05003

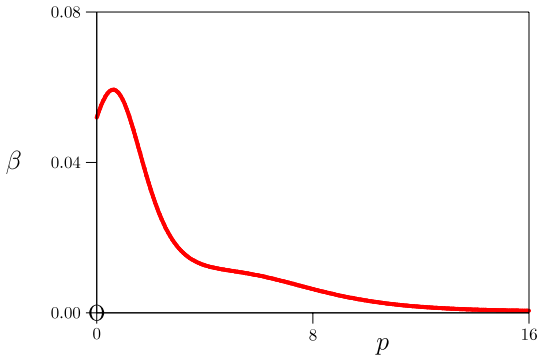

Figure 8. Compressibility of the minimal lattice knot of type 3_1^+ with volume V_e in the SC lattice.

case in figure 2. The pressure range on the X-axis is also expanded to larger pressure (up to $p = 16$ in this case, compared to $p = 4$ in figure 2). The qualitative shape of the curve is also slightly changed; there is still a global maximum at a non-zero value of p, but the secondary local maximum has disappeared. Nevertheless, the general shape of the curve is comparable to the curve in figure 2. The global maximum is at $p = 0.610\,46\cdots$ where $\beta = 0.059\,07\cdots$.

The maximum amount of useful work that can be performed by letting a lattice knot type 3_1^+ expand from its minimal containing volume to its equilibrium at zero pressure can be computed from the free energy of the model. If the volume V_b is used, then $\mathcal{F}_{SC}(3_1^+) = -\log \mathcal{Z}_{SC}(3_1^+)$ with the partition function given by equation (2).

By identifying the smallest value of V_b in equation (2), putting $p = 0$ and determining the free energy difference between the compressed and zero pressure states, it follows that the maximum amount of useful work is $\mathcal{W}_{3_1^+} = \log 1664 - \log 12 = \log(416/3) = 4.932\,07\cdots$. Interestingly, in this case the same result is obtained if one uses the average excluded volume instead.

3.2.2. Compressibility of 4_1. The compressibility of the figure of eight knot 4_1 is illustrated in figure 9: in figure 9(a) the compressibility in a rectangular box volume V_b is shown, and in figure 9(b) the compressibility in an average excluded volume V_e is illustrated. Note the different scales on the axes of the two graphs. One may similarly determine the maximum amount of useful work if the lattice knot is relaxed from its smallest containing volume to its state at zero pressure. If the volume V_b is used, then this is $\mathcal{W}_{4_1} = \log(38/9) = 1.440\,36\cdots$, and if V_e is used, then $\mathcal{W}_{4_1} = \log 38 = 3.637\,59\cdots$.

3.2.3. Compressibilities of 5_1^+ *and* 5_2^+. The compressibilities of the two knots 5_1^+ and 5_2^+ are plotted in figure 10. For both choices of the volumes, the knot 5_2^+ is more compressible than 5_1^+. The generic shapes of the compressibility of 5_2^+ are similar for the two volumes, both cases having a global maximum away from zero pressure. In the case of 5_1^+, on the other hand, the global maximum in the compressibility is at zero pressure when the volume V_b is used, but it is at $p > 0$ when V_e is used. The maxima in figure 10(a) are at $p = 0$ ($\beta = 0.826\,95\cdots$) for 5_1^+ and $p = 0.132\,37\cdots$ ($\beta = 1.222\,94\cdots$) for 5_2^+. Observe that 5_1^+ has a local maximum at $p = 1.436\,22\cdots$ ($\beta = 0.032\,60\cdots$). In figure 10(b) the

J. Stat. Mech. (2012) P05003

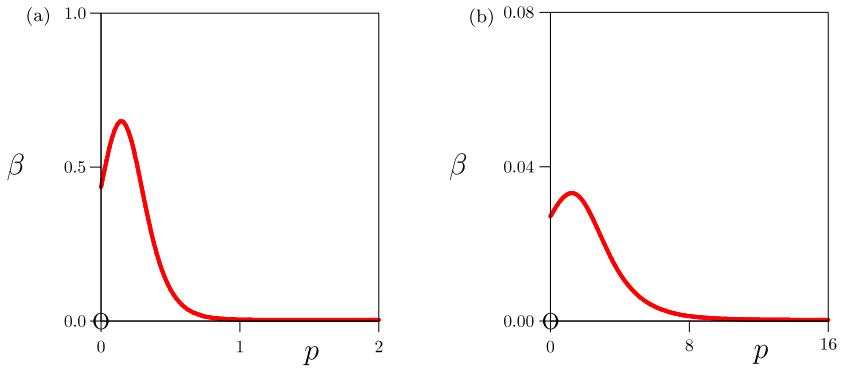

Figure 9. Compressibility of the minimal lattice knot of type 4_1 in the SC lattice. (a) Compressibility in a rectangular box volume V_b. (b) Compressibility in an average excluded volume V_e.

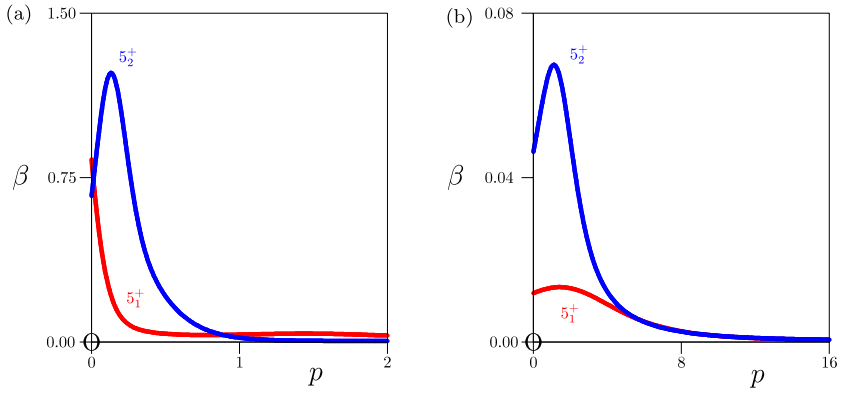

Figure 10. Compressibilities of the minimal lattice knots of types 5_1^+ and 5_2^+ in the SC lattice. (a) Compressibilities in a rectangular box volume V_b. (b) Compressibilities in an average excluded volume V_e.

global maxima are located at $p = 1.438\,11\cdots$ ($\beta = 0.013\,08\cdots$) and $p = 1.111\,77\cdots$ ($\beta = 0.067\,18\cdots$) respectively.

The maximum amounts of work that can be extracted from these two knot types are as follows: for 5_1^+, $\mathcal{W}_{5_1^+} = \log(139/5) = 3.325\,04\cdots$ with volume V_b and $\mathcal{W}_{5_1^+} = \log 139 = 4.934\,47\cdots$ with volume V_e, and for 5_2^+, $\mathcal{W}_{5_2^+} = \log(133/5) = 3.280\,91\cdots$ with volume V_b and $\mathcal{W}_{5_2^+} = \log 2394 = 7.780\,72\cdots$ with volume V_e.

3.2.4. Compressibilities of knots with six crossings. The compressibilities of knots with six crossings are displayed in figure 11. For both choices of V_b and V_e as containing volumes, the knots 6_3 were most compressible, and 6_1^+ least compressible.

In all three cases the maximal compressibility was at non-zero pressure, and only in the case of 6_2^+ with volume V_b did we observe a local maximum in the compressibility at higher pressure, compared to the global maximum at low pressure. By using the volume V_b to measure the compressibility, the (global) maxima in the compressibility were at $p = 0.229\,58\cdots$ where $\beta = 0.818\,16\cdots$ for 6_1^+, at $p = 0.091\,03\cdots$ where $\beta = 0.945\,24\cdots$

J. Stat. Mech. (2012) P05003

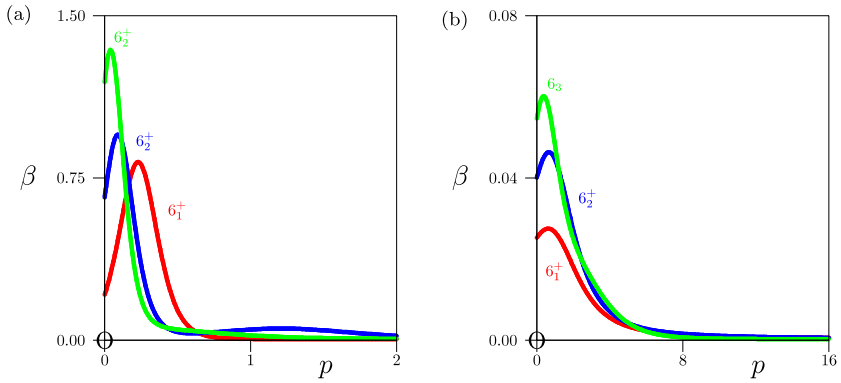

Figure 11. Compressibilities of the minimal lattice knots of types 6_1^+, 6_2^+ and 6_3 in the SC lattice. (a) Compressibilities in a rectangular box volume V_b. (b) Compressibilities in an average excluded volume V_e.

for 6_2^+ (with a local maximum at $p = 1.209\,77\cdots$ where $\beta = 0.048\,40\cdots$), and at $p = 0.041\,18\cdots$ where $\beta = 1.337\,19\cdots$ for 6_3.

The maximum amounts of work that can be extracted from these knot types are $\mathcal{W}_{6_1^+} = \log(128/9) = 2.654\,81\cdots$, $\mathcal{W}_{6_2^+} = \log 171 = 5.141\,66\cdots$, and $\mathcal{W}_{6_3} = \log(74/9) = 2.106\,84\cdots$.

Using the volume V_e instead, one finds the global maxima at $p = 0.617\,67\cdots$ where $\beta = 0.027\,23\cdots$ for 6_1^+, at $p = 0.660\,97\cdots$ where $\beta = 0.046\,09\cdots$ for 6_2^+, and at $p = 0.373\,98\cdots$ where $\beta = 0.059\,88\cdots$ for 6_3.

The maximum amounts of work that can be extracted from these knot types are $\mathcal{W}_{6_1^+} = \log 256 = 5.545\,17\cdots$, $\mathcal{W}_{6_2^+} = \log(36/19) = 6.527\,95\cdots$, and $\mathcal{W}_{6_3} = \log 74 = 4.304\,06\cdots$.

3.2.5. Compressibilities of knots with seven or more crossings. The compressibilities of knots with seven and eight crossings for the choice V_b are summarized in table 3. Several minimal lattice knots in table 3 are incompressible, for example 0_1, 7_3^+, 8_5^+, 8_6^+, and so on. The largest compressibility at zero pressure is for the knot 8_3, and this is also the largest compressibility overall in the table. In this table the appearance of a local maximum in the compressibility, as seen for the trefoil in figure 2, for example, appears to be the

Table 3. Compressibilities of SC lattice knots with volume V_b.

Knot	$\beta(0)$	p_m	max $\beta(p)$	loc p_m	loc max $\beta(p)$	$\mathcal{W}_K$	min V_b
0_1	0	—	—	—	—	0	0
3_1^+	0.653 47	0.135 57	0.928 45	1.821 15	0.058 88	4.932 07	16
4_1	0.432 28	0.145 99	0.646 17	—	—	1.440 36	27
5_1^+	0.826 95	0	0.826 95	1.436 22	0.032 60	3.325 04	30
5_2^+	0.661 16	0.132 37	1.222 94	—	—	3.280 91	30
6_1^+	0.205 46	0.229 58	0.818 16	—	—	2.654 81	36
6_2^+	0.654 97	0.091 03	0.945 25	1.209 77	0.048 40	5.14166	45
6_3	1.188 46	0.041 19	1.337 19	—	—	2.106 84	45

Table 3. (Continued.)

Knot	$\beta(0)$	p_m	max $\beta(p)$	loc p_m	loc max $\beta(p)$	$\mathcal{W}_K$	min V_b
7_1^+	1.434 10	0.065 58	1.936 27	—	—	1.551 10	40
7_2^+	1.565 22	0	1.565 22	—	—	2.761 17	45
7_3^+	0	—	—	—	—	0	45
7_4^+	0.053 40	0	0.053 40	—	—	0.336 47	60
7_5^+	0.116 67	0.231 79	1.280 10	—	—	5.283 20	45
7_6^+	0.973 33	0.037 59	1.075 80	—	—	2.181 83	60
7_7^+	0.761 90	0.050 29	0.891 65	—	—	1.098 61	64
8_1^+	1.311 69	0.046 11	1.494 28	—	—	3.564 49	48
8_2^+	2.493 40	0	2.493 40	—	—	4.610 42	48
8_3	3.981 58	0	3.981 58	—	—	2.121 93	27
8_4^+	0.234 41	0.183 60	1.037 28	—	—	3.685 87	60
8_5^+	0	—	—	—	—	0	80
8_6^+	0	—	—	—	—	0	80
8_7^+	0	—	—	—	—	0	60
8_8^+	0	—	—	—	—	0	80
8_9	0.608 41	0.099 61	1.435 94	—	—	1.994 70	60
8_{10}^+	0	—	—	—	—	0	80
8_{11}^+	0	—	—	—	—	0	80
8_{12}	1.212 12	0.041 85	1.435 94	—	—	1.098 61	60
8_{13}^+	1.789 04	0	1.789 04	—	—	1.626 12	64
8_{14}^+	0	—	—	—	—	0	80
8_{15}^+	2.365 53	0	2.365 53	—	—	4.450 76	48
8_{16}^+	0	—	—	—	—	0	80
8_{17}	1.269 59	0.042 60	1.431 08	—	—	3.544 58	64
8_{18}	0	—	—	—	—	0	100
8_{19}^+	1.169 78	0.045 25	1.349 59	—	—	2.091 52	45
8_{20}^+	0	—	—	—	—	0	60
8_{21}^+	0.362 79	0.155 14	0.955 39	—	—	2.330 82	48
9_1^+	2.991 29	0	2.991 29	—	—	1.620 95	50
9_2^+	1.970 47	0	1.970 47	0.401 39	0.600 45	7.394 88	48
9_{42}^+	0.803 92	0	0.803 92	—	—	2.004 59	60
9_{47}^+	1.813 76	0	1.813 76	—	—	0.262 36	80
10_1^+	1.660 66	0	1.660 66	0.189 95	0.983 20	6.976 24	54
10_2^+	3.126 85	0	3.126 85	—	—	4.570 09	60

exception, rather than the rule. Only the knot types 3_1^+, 5_1^+, 6_2^+, 9_2^+ and 10_1^+ have local maxima in their compressibilities when pressurized in a rectangular box. Most knot types have maximum useful work between 0 and 3 in lattice units, but for the knot types 3_1^+, 6_2^+, 7_5^+, 8_2^+, 8_{15}^+, 9_2^+, 10_1^+ and 10_2^+ this exceeds 4 lattice units.

The minimal values of V_b are listed in the last column of table 3. This shows, for example, that a trefoil can be tied in the cubic lattice in a rectangular box of volume 16. Comparison of the results in this list shows that amongst six crossing knots it is 6_1^+ which

J. Stat. Mech. (2012) P05003

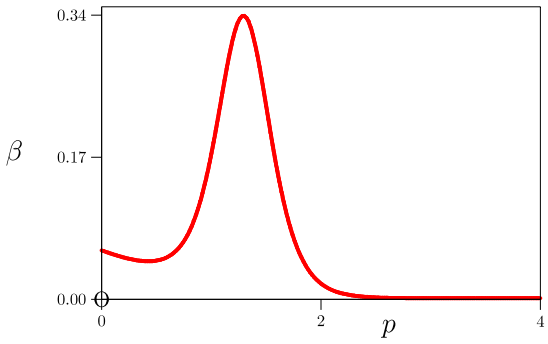

Figure 12. Compressibility of the SC minimal lattice knot of type 10_1^+ in its average excluded volume V_e.

can be tied in the smallest box, and amongst seven crossing knots 7_1^+. In the list of eight crossing prime knots, type 8_3 can be tied in a box of volume 27, far smaller than any other eight crossing knot (or even any five, six or seven crossing knot). This suggests that 8_3 can be embedded very efficiently, using relatively little volume, in the SC lattice.

In table 4 the compressibilities of minimal SC lattice knots with the choice of the volume V_e are displayed. Generally, the compressibilities are smaller than those in table 3—this is to be expected because the average excluded volume V_e is a more tightly fitting volume about the lattice knots, compared to the rectangular box volume V_b. All the minimal lattice knots in table 4 are compressible, with the exception of the unknot and the knot type 8_7^+. The largest compressibility is obtained for knot type 10_1^+ at $p = 1.292\,56\cdots$ where $\beta = 0.337\,99\cdots$. In knot types such as 10_1^+, the compressibility varies dramatically with pressure, and this example is illustrated in figure 12. A similar profile can be plotted for 9_{47}^+. The largest compressibility at zero pressure is found for knot type 10_2^+. Observe that there are no knot types with a secondary local maximum in the compressibility in table 4. Most knot types have maximum useful work between 0 and 6 in lattice units, but

Table 4. Compressibilities of SC lattice knots with volume V_e.

Knot	$\beta(0)$	p_m	max $\beta(p)$	loc p_m	loc max $\beta(p)$	$\mathcal{W}_K$	min V_e
0_1	0	—	—	—	—	0	0
3_1^+	0.051 67	0.610 46	0.059 07	—	—	4.932 07	8
4_1	0.026 84	1.227 31	0.032 90	—	—	3.637 59	12
5_1^+	0.011 59	1.438 11	0.013 08	—	—	4.934 47	14
5_2^+	0.046 00	1.111 77	0.067 18	—	—	7.780 72	44/3
6_1^+	0.025 00	0.617 68	0.027 24	—	—	5.545 18	37/2
6_2^+	0.039 82	0.660 98	0.046 09	—	—	6.527 96	113/6
6_3	0.054 38	0.373 98	0.059 89	—	—	4.304 07	37/2
7_1^+	0.037 48	0.150 97	0.037 87	—	—	6.561 74	121/6
7_2^+	0.050 04	0.021 86	0.050 05	—	—	8.854 74	85/4
7_3^+	0.003 54	0.536 00	0.003 57	—	—	2.302 59	65/3
7_4^+	0.007 06	0.938 23	0.008 19	—	—	1.252 76	68/3

J. Stat. Mech. (2012) P05003

Table 4. (Continued.)

Knot	$\beta(0)$	p_m	max $\beta(p)$	loc p_m	loc max $\beta(p)$	$\mathcal{W}_K$	min V_e
7_5^+	0.013 11	1.959 42	0.042 74	—	—	5.283 20	68/3
7_6^+	0.037 11	0	0.037 11	—	—	5.870 71	143/6
7_7^+	0.030 62	0.560 27	0.038 59	—	—	1.658 23	139/6
8_1^+	0.069 28	0	0.069 28	—	—	6.203 55	73/3
8_2^+	0.075 73	0	0.075 73	—	—	7.554 86	293/12
8_3	0.026 84	1.227 31	0.032 90	—	—	3.637 59	12
8_4^+	0.034 88	0.536 31	0.038 40	—	—	6.211 60	311/12
8_5^+	0.011 02	0.085 09	0.011 03	—	—	3.178 05	167/6
8_6^+	0.011 69	0.634 70	0.012 26	—	—	5.438 08	167/6
8_7^+	0	—	—	—	—	0	77/3
8_8^+	0.017 58	0	0.017 58	—	—	3.481 24	57/2
8_9	0.046 20	0.551 86	0.059 06	—	—	6.599 87	79/3
8_{10}^+	0.009 35	0.478 16	0.009 54	—	—	3.555 35	28
8_{11}^+	0.002 99	0.017 57	0.002 99	—	—	0.693 15	169/6
8_{12}	0.016 39	0.477 43	0.017 09	—	—	3.988 98	83/3
8_{13}^+	0.054 87	0.179 77	0.055 81	—	—	6.298 95	161/6
8_{14}^+	0.005 14	0.231 52	0.005 16	—	—	2.708 05	169/6
8_{15}^+	0.057 97	0.778 10	0.079 90	—	—	7.421 18	76/3
8_{16}^+	0.003 67	0.016 53	0.003 67	—	—	0.693 15	359/12
8_{17}	0.032 36	1.336 62	0.036 86	—	—	5.624 02	343/12
8_{18}	0.017 20	0.531 64	0.017 97	—	—	3.610 92	377/12
8_{19}^+	0.066 51	0.474 15	0.086 67	—	—	6.368 19	107/6
8_{20}^+	0.002 91	0.602 79	0.002 98	—	—	1.609 44	275/12
8_{21}^+	0.051 77	0.544 28	0.055 10	—	—	7.062 62	263/12
9_1^+	0.070 13	0.311 27	0.077 55	—	—	8.882 88	103/4
9_2^+	0.048 25	0.666 53	0.052 75	—	—	11.132 55	169/6
9_{42}^+	0.023 16	0.121 42	0.023 12	—	—	6.361 30	289/12
9_{47}^+	0.022 59	1.157 83	0.192 59	—	—	5.655 99	101/4
10_1^+	0.057 28	1.292 56	0.337 99	—	—	9.173 47	83/3
10_2^+	0.078 93	0	0.078 93	—	—	9.113 39	377/12

for the knot types 5_2^+, 6_2^+, 7_1^+, 7_2^+, 8_1^+, 8_2^+, 8_4^+, 8_9, 8_{13}^+, 8_{15}^+, 8_{19}^+, 8_{21}^+, 9_1^+, 9_2^+, 10_1^+ and 10_2^+ this exceeds 6 lattice units. The knot type 9_2^+ has a particularly large value for the work, namely $\mathcal{W}_{9_2^+} = 11.132\,55\cdots$, far larger than types 10_1^+ and 10_2^+, where the work exceeds 9 units.

The minimal values of V_e are listed in the last column of table 4. The minimal value for 3_1^+ is 8, which is only one half of the volume of the minimal size rectangular box containing a lattice knot of type 3_1^+. This shows that the volume V_e is far smaller than V_b for this knot type, and the average excluded volume of the knot type is a far tighter fit about the lattice knot. Comparison of the results in this list shows similarly that 8_3 can be tied with a relatively very small value of V_e, in this case $V_e = 12$, smaller than the minimal value of V_e for any other five, six, seven or eight crossing minimal lattice knot.

J. Stat. Mech. (2012) P05003

Table 5. Partition functions: minimal FCC lattice knots pressurized in a rectangular box.

Knot	$Z_n(p)$
0_1	8
3_1^+	$16e^{-27p} + 48e^{-24p}$
4_1	$24e^{-64p} + 576e^{-48p} + 348e^{-45p} + 1416e^{-36p} + 192e^{-32p} + 48e^{-30p} + 192e^{-27p}$
5_1^+	$48e^{-48p} + 24e^{-45p} + 24e^{-36p}$
5_2^+	$48e^{-80p} + 96e^{-64p} + 192e^{-60p} + 288e^{-48p} + 96e^{-45p} + 48e^{-40p}$
6_1^+	$48e^{-125p} + 816e^{-100p} + 144e^{-96p} + 4224e^{-80p} + 1104e^{-75p} + 912e^{-72p} + 2448e^{-64p} + 5712e^{-60p} + 816e^{-54p} + 2112e^{-48p} + 624e^{-45p} + 48e^{-40p}$
6_2^+	$960e^{-80p} + 288e^{-75p} + 48e^{-72p} + 864e^{-64p} + 1344e^{-60p} + 1152e^{-48p} + 384e^{-45p}$
6_3	$960e^{-100p} + 48e^{-96p} + 18\,336e^{-80p} + 4896e^{-75p} + 1440e^{-72p} + 24\,096e^{-64p} + 24\,864e^{-60p} + 96e^{-54p} + 23\,280e^{-48p} + 3840e^{-45p} + 864e^{-36p}$
7_1^+	$336e^{-100p} + 2400e^{-80p} + 144e^{-75p} + 96e^{-72p} + 192e^{-64p} + 864e^{-60p} + 48e^{-54p}$
7_2^+	$48e^{-120p} + 432e^{-100p} + 96e^{-96p} + 96e^{-90p} + 1200e^{-80p} + 552e^{-75p} + 432e^{-72p} + 336e^{-64p} + 672e^{-60p} + 168e^{-54p} + 96e^{-45p}$
7_3^+	$96e^{-100p} + 96e^{-96p} + 288e^{-80p} + 96e^{-75p} + 144e^{-72p} + 48e^{-64p} + 192e^{-60p}$
7_4^+	$72e^{-100p} + 24e^{-96p}$
7_5^+	$144e^{-125p} + 624e^{-120p} + 6192e^{-100p} + 1920e^{-96p} + 720e^{-90p} + 8112e^{-80p} + 2544e^{-75p} + 1488e^{-72p} + 2064e^{-64p} + 3216e^{-60p} + 432e^{-54p}$
7_6^+	$480e^{-100p} + 1728e^{-80p} + 96e^{-75p} + 1728e^{-64p} + 288e^{-60p} + 576e^{-48p}$
7_7^+	$96e^{-100p} + 384e^{-80p} + 48e^{-72p} + 384e^{-64p} + 192e^{-60p} + 192e^{-48p}$

3.3. Compressibilities of minimal lattice knots in the FCC and BCC lattices

The compressibilities of minimal lattice knots in the FCC lattice can similarly be computed, using again two choices of an enclosing volume, namely V_b for the volume of the minimal rectangular box containing the polygon, and V_e for the average excluded volume.

The partition functions of FCC minimal lattice knots up to crossing number seven and with volumes V_b are listed in table 5. With the choice of the average excluded volume the partition functions are similarly more complicated, and we do not reproduce them here.

The partition functions of minimal lattice knots in the BCC lattice with the volume V_b are similarly given in table 6. Far more lengthy expressions are obtained when the average excluded volume V_e is used.

3.3.1. Compressibilities of 3_1^+ in the FCC and BCC lattices. Considering first the cases with the rectangular box volume V_b, the partition functions of minimal length lattice trefoils in the FCC and BCC lattices evaluate to

$$\mathcal{Z}_{\mathrm{FCC}}(3_1^+) = 16e^{-27p} + 48e^{-24p};$$
$$\mathcal{Z}_{\mathrm{BCC}}(3_1^+) = 24e^{-125p} + 480e^{-100p} + 696e^{-80p} + 384e^{-75p}.$$

J. Stat. Mech. (2012) P05003

Table 6. Partition functions: minimal BCC lattice knots pressurized in a rectangular box.

Knot	$Z_n(p)$
0_1	$6e^{-8p} + 6e^{-4p}$
3_1^+	$24e^{-125p} + 480e^{-100p} + 696e^{-80p} + 384e^{-75p}$
4_1	$12e^{-80p}$
5_1^+	$48e^{-210p} + 624e^{-180p} + 792e^{-175p} + 432e^{-168p} + 4896e^{-150p} + 1776e^{-144p} + 2736e^{-140p} + 264e^{-125p} + 1536e^{-120p} + 504e^{-112p} + 456e^{-108p} + 768e^{-105p}$
5_2^+	$144e^{-180p} + 144e^{-175p} + 2064e^{-150p} + 48e^{-144p} + 912e^{-140p} + 24e^{-125p} + 1056e^{-120p} + 480e^{-112p}$
6_1^+	$48e^{-150p} + 24e^{-112p}$
6_2^+	$336e^{-216p} + 3600e^{-180p} + 576e^{-175p} + 3168e^{-150p} + 432e^{-144p} + 144e^{-125p}$
6_3	$48e^{-210p} + 528e^{-180p} + 240e^{-168p} + 1968e^{-150p} + 336e^{-144p} + 144e^{-125p} + 48e^{-120p}$
7_1^+	$24e^{-252p} + 144e^{-216p} + 144e^{-210p} + 936e^{-180p} + 216e^{-175p}$
7_2^+	$24e^{-180p}$
7_3^+	$48e^{-294p} + 480e^{-252p} + 144e^{-245p} + 1632e^{-240p} + 144e^{-225p} + 720e^{-216p} + 9312e^{-210p} + 4128e^{-200p} + 3000e^{-180p} + 1152e^{-175p} + 384e^{-168p} + 816e^{-160p} + 48e^{-150p} + 480e^{-144p}$
7_4^+	$24e^{-343p} + 480e^{-294p} + 2016e^{-252p} + 1008e^{-245p} + 912e^{-216p} + 2592e^{-210p} + 144e^{-196p} + 48e^{-192p} + 2544e^{-180p} + 1008e^{-175p} + 48e^{-168p} + 384e^{-150p}$
7_5^+	$48e^{-252p} + 192e^{-240p} + 144e^{-225p} + 144e^{-216p} + 1872e^{-210p} + 1632e^{-200p} + 2688e^{-180p} + 528e^{-175p} + 192e^{-168p} + 816e^{-160p} + 48e^{-150p} + 480e^{-144p}$
7_6^+	$48e^{-150p}$
7_7^+	$24e^{-144p}$

The expected volumes of the lattice minimal knot at pressure p are

$$\langle V_{\mathrm{b}}\rangle = 3\left[\frac{e^{-51p}}{(3e^{-27p} + 8e^{-24p})(e^{-27p} + 3e^{-24p})}\right]$$

in the FCC lattice and

$$\langle V_{\mathrm{b}}\rangle = 5\left[\frac{25e^{-125p} + 400e^{-100p} + 464e^{-80p} + 240e^{-75p}}{e^{-125p} + 20e^{-100p} + 29e^{-80p} + 16e^{-75p}}\right]$$

in the BCC lattice.

The compressibilities in these cases are given by

$$\beta = 3\left[\frac{e^{-51p}}{(3e^{-27p} + 8e^{-24p})(e^{-27p} + 3e^{-24p})}\right]$$

in the FCC lattice and

$$\beta = 5\left[\frac{500e^{-225p} + 2349e^{-205p} + 1600e^{-200p} + 9280e^{-180p} + 8000e^{-175p} + 464e^{-155p}}{(25e^{-125p} + 400e^{-100p} + 464e^{-80p} + 240e^{-75p})A}\right]$$

in the BCC lattice, where $A = (e^{-125p} + 20e^{-100p} + 29e^{-80p} + 16e^{-75p})$.

doi:10.1088/1742-5468/2012/05/P05003

J. Stat. Mech. (2012) P05003

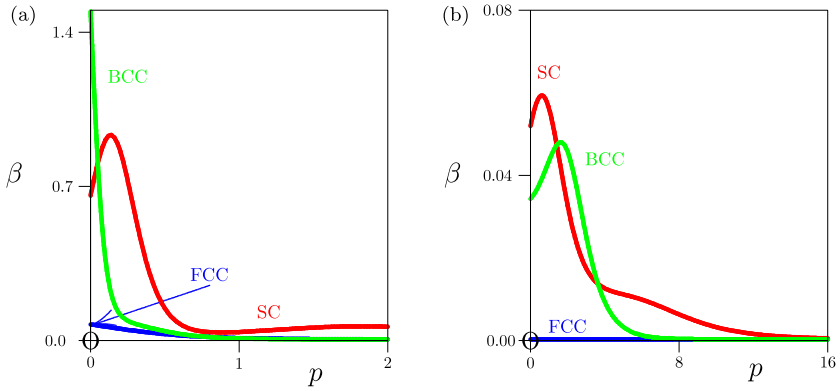

Figure 13. Compressibilities of the minimal lattice knots of type 3_1^+ in the FCC and BCC lattices. The compressibilities in the SC lattice (see figures 2 and 8) are included for comparison. (a) Compressibilities in a rectangular box volume V_b. (b) Compressibilities in an average excluded volume V_e.

Plotting these compressibilities in the FCC and BCC lattices for $p \in [0, 2]$ gives the curves in figure 13. If the average excluded volume V_e is used instead, then the partition functions of minimal length lattice trefoils in the FCC and BCC lattices are

$$\mathcal{Z}_{\mathrm{FCC}}(3_1^+) = 64\mathrm{e}^{-13/2p}; \tag{4}$$

$$\begin{aligned}\mathcal{Z}_{\mathrm{BCC}}(3_1^+) = {} & 168\mathrm{e}^{-16p} + 240\mathrm{e}^{-52/3p} + 432\mathrm{e}^{-50/3p} + 144\mathrm{e}^{-53/3p} \\ & + 288\mathrm{e}^{-17p} + 72\mathrm{e}^{-18p} + 96\mathrm{e}^{-55/3p} + 24\mathrm{e}^{-56/3p} \\ & + 96\mathrm{e}^{-47/3p} + 24\mathrm{e}^{-44/3p}.\end{aligned} \tag{5}$$

The expected volume of the minimal lattice trefoil at pressure p is equal to $\langle V_\mathrm{e}\rangle = 13/2$ (independent of p) in the FCC lattice, and is a lengthy expression (dependent on p) in the BCC lattice. The compressibility in the FCC lattice is identically zero, and in the BCC lattice is again a lengthy expression. Plotting these compressibilities in the FCC and BCC lattices for $p \in [0, 2]$ gives the curves in figure 13(b).

Observe that for both choices of the volumes V_b and V_e, 3_1^+ is more compressible in the BCC lattice than in the FCC lattice. This observation shows that the knot is much more tightly embedded in the FCC lattice, and that increasing pressure compresses the knot less in the FCC lattice.

The global maxima of β in figure 13(a) (this is for the choice V_b) occur at $p = 0$ in the FCC and BCC lattices. In this particular case, $\beta = 1.176\,90\cdots$ in the FCC lattice and $\beta = 1.489\,18\cdots$ in the BCC lattice at zero pressure. The compressibility decreases monotonically with increasing $p > 0$ in both cases. If the volume V_e is used instead, then $\beta = 0$ for $p \geq 0$ in the FCC lattice (the lattice knot is incompressible), but there is a global maximum in β at $p = 1.624\,52\cdots$ where $\beta = 0.047\,73\cdots$.

The maximum amounts of useful work that can be performed by letting a lattice knot type 3_1^+ expand from its maximal compressed state to its equilibrium at zero pressure in the FCC and BCC lattices can be computed as before. In these lattices,

J. Stat. Mech. (2012) P05003

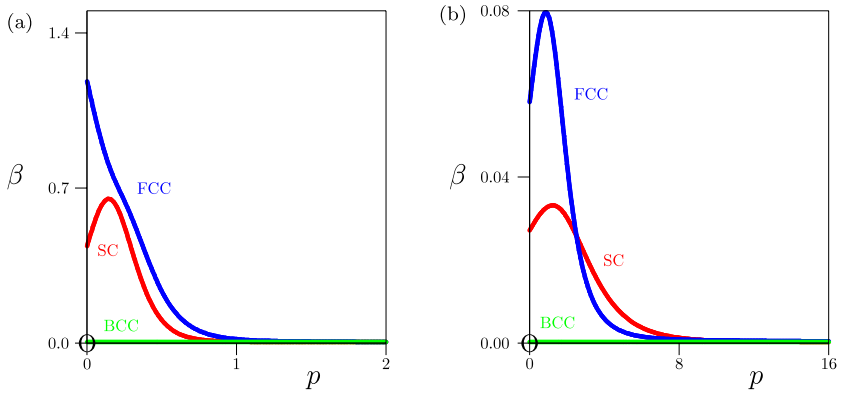

Figure 14. Compressibilities of the minimal lattice knots of type 4_1 in the FCC and BCC lattices. The compressibilities in the SC lattice (see figure 9) are included for comparison. (a) Compressibilities in a rectangular box volume V_b. (b) Compressibilities in an average excluded volume V_e.

$\mathcal{W}_{3_1^+} = \log(4/3) = 0.287\,68\cdots$ in the FCC lattice, and $\mathcal{W}_{3_1^+} = \log(33/8) = 1.417\,07\cdots$ in the BCC lattice. If V_e is used instead, then $\mathcal{W}_{3_1^+} = 0$ in the FCC lattice, and $\mathcal{W}_{3_1^+} = \log 66 = 4.189\,65\cdots$ in the BCC lattice.

3.3.2. The compressibilities of minimal lattice knots in the FCC and BCC lattices. The compressibilities of the figure of eight knot 4_1 are illustrated in the FCC and BCC lattices for the choices of the volume V_b and V_e in figure 14. For the choice of volume V_b in the FCC lattice, the maximum compressibility of 4_1 is at $p = 0$, where $\beta = 1.176\,90\cdots$, but for V_e one obtains a maximum at $p = 0.863\,18\cdots$ where $\beta = 0.079\,38\cdots$. The knot is incompressible for both choices V_b and V_e in the BCC lattice.

The maximum amounts of work are $\mathcal{W}_{4_1} = \log(233/16) = 2.678\,44\cdots$ in the FCC lattice for V_b, and $\mathcal{W}_{4_1} = \log(233/8) = 3.371\,59\cdots$ in the FCC lattice with the choice V_e.

Data on the compressibilities of lattice knots in the FCC lattice with the choice of volume V_b are given in table 7 and with the choice of volume V_e in table 8. Observe that in most cases the maximal compressibility is at zero pressure, and that exceptions to this are sporadic in tables 7 and 8. Even more sporadic are knot types with secondary local maxima in the compressibility, as seen for example in figure 2 for the trefoil knot—in fact, with the choice of volume V_b only the knot types 7_1^+ and 8_{11}^+ have secondary local maxima in the compressibility, and with V_e, only 8_{18}.

Amongst eight crossing knot types the knot types 8_{18}, 8_{19}^+ and 8_{20}^+ can be realized in a rectangular box of volume 45, small compared with the other eight crossing knots. This is only slightly smaller than the minimum value of V_b for 8_1^+, which is 48.

The maximum work in table 7 is obtained for 8_1^+, and $\mathcal{W}_{8_1^+} = 8.447\,79\cdots$. Other knot types which have high values for $\mathcal{W}_K$ are 6_1^+, 8_2^+, 8_{11}^+, 8_{13}^+, 8_{20}^+ and 9_2^+.

If one considers the volume V_e instead, then there is a steady increase of V_e with increasing knot complexity in table 8. The maximum work in table 8 is obtained for 8_1^+, and $\mathcal{W}_{8_1^+} = 9.140\,94\cdots$. Other knot types which have high values for $\mathcal{W}_K$ are 6_3, 8_2^+, 8_{11}^+, 8_{13}^+, 9_2^+ and 10_1^+.

J. Stat. Mech. (2012) P05003

Table 7. Compressibilities of FCC lattice knots with volume V_b.

Knot	$\beta(0)$	p_m	max $\beta(p)$	loc p_m	loc max $\beta(p)$	$\mathcal{W}_K$	min V_b
0_1	0	—	—	—	—	0	0
3_1^+	0.068 18	0	0.068 18	—	—	0.287 68	24
4_1	1.176 90	0	1.176 90	—	—	2.678 45	27
5_1^+	0.546 61	0.10381	0.729 40	—	—	1.386 29	36
5_2^+	1.840 36	0	1.840 36	—	—	2.772 59	40
6_1^+	2.781 10	0	2.781 10	—	—	5.981 41	40
6_2^+	2.285 12	0	2.285 12	—	—	2.574 52	45
6_3	2.313 50	0	2.313 50	—	—	4.778 19	36
7_1^+	1.631 06	0.02343	1.650 22	0.462 11	0.170 66	4.442 65	54
7_2^+	2.631 44	0	2.631 44	—	—	3.761 20	45
7_3^+	2.102 33	0	2.102 33	—	—	1.609 44	60
7_4^+	0.030 30	0.27976	0.040 82	—	—	1.386 29	96
7_5^+	2.865 02	0	2.865 02	—	—	4.151 91	54
7_6^+	2.776 93	0	2.776 93	—	—	2.140 07	48
7_7^+	2.793 74	0	2.793 74	—	—	1.909 54	48
8_1^+	3.548 11	0	3.548 11	—	—	8.447 79	48
8_2^+	3.086 99	0	3.086 99	—	—	5.593 06	54
8_3	3.398 70	0	3.398 70	—	—	3.101 09	60
8_4^+	3.354 18	0	3.354 18	—	—	3.756 54	60
8_5^+	1.219 29	0	1.219 29	—	—	3.433 99	63
8_6^+	3.924 41	0	3.924 41	—	—	3.080 89	60
8_7^+	1.618 60	0	1.618 60	—	—	1.466 34	64
8_8^+	2.825 49	0	2.825 49	—	—	2.063 69	60
8_9	3.132 20	0	3.132 20	—	—	2.602 69	60
8_{10}^+	2.037 27	0	2.037 27	—	—	0.810 93	80
8_{11}^+	3.107 30	0	3.107 30	0.583 72	0.189 36	8.040 93	54
8_{12}	3.149 59	0.008 38	3.162 25	—	—	2.656 76	60
8_{13}^+	3.252 99	0	3.252 99	—	—	5.249 65	48
8_{14}^+	3.073 91	0	3.073 91	—	—	2.126 13	60
8_{15}^+	2.671 95	0	2.671 95	—	—	4.840 24	60
8_{16}^+	1.885 07	0	1.885 07	—	—	1.216 40	64
8_{17}	1.816 76	0	1.816 76	—	—	1.216 40	64
8_{18}	3.116 96	0.015 03	3.167 90	—	—	3.289 16	45
8_{19}^+	0.258 69	0.177 60	1.501 98	—	—	3.135 49	45
8_{20}^+	1.732 55	0	1.732 55	—	—	5.955 51	45
8_{21}^+	2.068 97	0	2.068 97	—	—	2.392 53	60
9_1^+	2.000 00	0.010 14	2.020 41	—	—	1.386 29	80
9_2^+	3.823 35	0	3.823 35	—	—	5.215 77	60
9_{42}^+	0	—	—	—	—	0	80
9_{47}^+	0.926 83	0.107 58	1.040 61	—	—	2.367 12	64
10_1^+	4.116 36	0	4.116 36	—	—	4.131 16	80
10_2^+	4.421 90	0	4.421 90	—	—	3.028 52	80

J. Stat. Mech. (2012) P05003

Table 8. Compressibilities of FCC lattice knots with volume V_e.

Knot	$\beta(0)$	p_m	max $\beta(p)$	loc p_m	loc max $\beta(p)$	$\mathcal{W}_K$	min V_e
0_1	0	—	—	—	—	0	0
3_1^+	0	—	—	—	—	0	13/2
4_1	0.057 73	0.863 18	0.079 39	—	—	3.371 60	61/6
5_1^+	0.017 93	1.003 05	0.023 93	—	—	1.386 29	37/3
5_2^+	0.028 08	0.395 66	0.028 99	—	—	2.772 59	85/6
6_1^+	0.054 61	0.188 26	0.055 25	—	—	5.981 41	101/6
6_2^+	0.061 28	0.572 04	0.077 99	—	—	4.653 96	33/2
6_3	0.038 45	1.339 26	0.075 23	—	—	6.975 41	107/6
7_1^+	0.037 63	1.239 06	0.059 85	—	—	4.442 65	56/3
7_2^+	0.042 19	0.811 00	0.055 25	—	—	4.454 35	41/2
7_3^+	0.020 67	0	0.020 67	—	—	2.995 73	22
7_4^+	0	—	—	—	—	0	59/3
7_5^+	0.045 97	0.831 34	0.065 70	—	—	6.349 14	127/6
7_6^+	0.028 78	0.608 37	0.031 74	—	—	4.624 97	23
7_7^+	0.007 06	0	0.007 06	—	—	2.602 69	149/6
8_1^+	0.071 31	0.833 33	0.083 79	—	—	9.140 94	68/3
8_2^+	0.078 10	0.709 37	0.111 84	—	—	7.097 14	70/3
8_3	0.054 29	0.248 97	0.055 68	—	—	5.991 46	51/2
8_4^+	0.077 84	0.647 40	0.133 05	—	—	6.059 12	23
8_5^+	0.035 90	0.056 11	0.035 94	—	—	4.820 28	27
8_6^+	0.050 98	0	0.050 98	—	—	5.278 11	157/6
8_7^+	0.017 14	1.001 29	0.027 88	—	—	3.258 10	80/3
8_8^+	0.021 33	0	0.021 33	—	—	4.143 13	82/3
8_9	0.038 62	0.996 43	0.058 10	—	—	4.682 13	76/3
8_{10}^+	0.017 19	0	0.017 19	—	—	3.583 52	55/2
8_{11}^+	0.045 65	0.904 66	0.056 86	—	—	8.734 08	76/3
8_{12}	0.042 10	0.508 00	0.049 37	—	—	5.141 66	82/3
8_{13}^+	0.054 85	0.938 25	0.083 29	—	—	8.650 85	149/6
8_{14}^+	0.021 99	1.486 54	0.026 28	—	—	6.345 64	167/6
8_{15}^+	0.034 77	0.539 93	0.037 77	—	—	6.632 00	163/6
8_{16}^+	0.024 06	0.345 59	0.024 90	—	—	5.780 74	85/3
8_{17}	0.011 95	0.630 42	0.012 46	—	—	4.682 13	29
8_{18}	0.048 95	0	0.048 95	0.850 36	0.046 79	6.061 75	85/3
8_{19}^+	0.016 21	1.023 91	0.019 49	—	—	3.135 49	56/3
8_{20}^+	0.050 23	0.984 38	0.080 07	—	—	6.243 20	59/3
8_{21}^+	0.025 66	1.255 37	0.037 51	—	—	5.918 89	133/6
9_1^+	0.007 58	0.034 10	0.007 58	—	—	1.386 29	86/3
9_2^+	0.072 79	0.673 16	0.081 13	—	—	8.473 87	161/6
9_{42}^+	0.000 28	0.020 07	0.000 28	—	—	0.693 15	149/6
9_{47}^+	0.011 77	0.457 73	0.011 90	—	—	4.158 88	89/3
10_1^+	0.066 85	0.554 16	0.079 21	—	—	7.389 26	31
10_2^+	0.063 72	0.451 45	0.083 70	—	—	5.225 75	32

J. Stat. Mech. (2012) P05003

Table 9. Compressibilities of BCC lattice knots with volume V_b.

Knot	$\beta(0)$	p_m	max $\beta(p)$	loc p_m	loc max $\beta(p)$	$\mathcal{W}_K$	min V_b
0_1	0.666 67	0.086 64	0.686 29	—	—	0.693 15	4
3_1^+	1.489 18	0	1.489 18	—	—	1.417 07	75
4_1	0	—	—	—	—	—	80
5_1^+	2.586 95	0.027 90	2.781 16	—	—	2.960 75	105
5_2^+	2.085 87	0.008 13	2.096 79	—	—	2.317 47	112
6_1^+	2.336 57	0.022 08	2.770 37	—	—	1.098 61	112
6_2^+	2.069 77	0	2.069 77	—	—	4.048 88	125
6_3	1.548 25	0	1.548 25	0.092 68	1.345 64	4.234 11	120
7_1^+	1.372 60	0	1.372 60	0.288 54	0.035 30	1.913 65	175
7_2^+	0	—	—	—	—	—	180
7_3^+	2.416 00	0.043 25	3.101 43	—	—	3.846 95	144
7_4^+	5.704 13	0	5.704 13	—	—	3.373 74	150
7_5^+	2.499 25	0.017 19	2.561 36	—	—	2.906 90	144
7_6^+	0	—	—	—	—	—	150
7_7^+	0	—	—	—	—	—	144
8_1^+	2.255 72	0.050 46	5.704 92	—	—	3.433 99	144
8_2^+	3.202 99	0	3.202 99	—	—	7.114 77	168
8_3	1.966 12	0.036 62	5.290 29	—	—	2.197 22	144
8_4^+	5.435 99	0	5.435 99	0.388 09	0.100 46	7.579 68	168
8_5^+	3.141 93	0	3.141 93	—	—	2.016 53	175
8_6^+	3.440 04	0	3.440 04	—	—	5.236 44	160
8_7^+	3.376 83	0	3.376 83	0.102 70	1.948 63	6.904 75	160
8_8^+	3.499 69	0	3.499 69	—	—	4.790 27	168
8_9	2.593 94	0	2.593 94	0.055 10	1.941 02	3.169 69	175
8_{10}^+	2.243 47	0	2.243 47	—	—	2.552 05	180
8_{11}^+	2.416 77	0	2.416 77	—	—	5.802 12	175
8_{12}	0	—	—	—	—	—	144
8_{13}^+	4.101 06	0	4.101 06	—	—	5.212 21	168
8_{14}^+	3.131 57	0	3.131 57	—	—	5.866 47	160
8_{15}^+	1.730 39	0.05233	2.126 01	—	—	3.390 02	168
8_{16}^+	0.979 28	0	0.979 28	—	—	1.299 28	175
8_{17}	0.928 79	0	0.928 79	—	—	0.305 38	180
8_{18}	4.706 75	0	4.706 75	0.163 92	2.023 37	6.599 87	144
8_{19}^+	1.692 40	0.03863	2.087 44	—	—	1.723 85	144
8_{20}^+	3.411 92	0	3.411 92	—	—	4.966 34	150
8_{21}^+	2.036 30	0	2.036 30	—	—	2.268 68	175
9_1^+	4.056 66	0	4.056 66	—	—	5.926 04	180
9_2^+	4.808 56	0	4.808 56	0.087 77	2.461 28	5.662 96	168
9_{42}^+	1.801 98	0	1.801 98	—	—	3.349 90	175
9_{47}^+	2.103 89	0	2.103 89	0.096 44	1.649 30	5.061 89	175
10_1^+	3.338 58	0	3.338 58	—	—	1.791 76	210
10_2^+	2.721 86	0.014 41	2.798 99	—	—	2.142 51	240

Data on the compressibility of lattice knots in the BCC lattice with the choice of volume V_b are given in table 9 and with the choice of volume V_e in table 10.

J. Stat. Mech. (2012) P05003

Table 10. Compressibilities of BCC lattice knots with volume V_e.

Knot	$\beta(0)$	p_m	max $\beta(p)$	loc p_m	loc max $\beta(p)$	$\mathcal{W}_K$	min V_e
0_1	0	—	—	—	—	0	0
3_1^+	0.034 02	1.624 52	0.047 73	—	—	4.189 65	44/3
4_1	0	—	—	—	—	0	64/3
5_1^+	0.065 53	1.228 54	0.102 45	—	—	5.327 88	80/3
5_2^+	0.056 74	0	0.056 74	—	—	4.620 06	91/3
6_1^+	0.006 29	0	0.006 29	—	—	0.405 47	35
6_2^+	0.052 41	0	0.052 41	1.372 61	0.037 55	5.147 49	116/3
6_3	0.038 92	0.790 96	0.056 19	—	—	4.234 11	116/3
7_1^+	0.037 48	0	0.037 48	—	—	1.712 98	124/3
7_2^+	0	—	—	—	—	0	44
7_3^+	0.063 47	0	0.063 47	0.220 71	0.061 15	6.149 54	134/3
7_4^+	0.098 45	0.576 90	0.381 84	—	—	5.453 18	40
7_5^+	0.069 12	0	0.069 12	—	—	5.209 49	48
7_6^+	0	—	—	—	—	0	47
7_7^+	0	—	—	—	—	0	48
8_1^+	0.090 74	0.232 62	0.112 79	—	—	2.740 84	49
8_2^+	0.092 47	0.719 50	0.178 08	—	—	7.807 92	152/3
8_3	0.008 56	0	0.008 56	—	—	0.587 79	152/3
8_4^+	0.133 67	0.395 42	0.260 81	—	—	6.886 53	148/3
8_5^+	0.071 55	0	0.071 55	—	—	5.036 95	167/3
8_6^+	0.069 02	0.655 04	0.107 83	—	—	5.236 44	54
8_7^+	0.080 47	0.579 10	0.131 55	—	—	6.904 75	52
8_8^+	0.115 40	0.465 46	0.115 58	—	—	6.582 03	54
8_9	0.064 12	0	0.064 12	—	—	4.779 12	169/3
8_{10}^+	0.042 89	0.772 48	0.055 74	—	—	5.442 42	166/3
8_{11}^+	0.070 35	0.937 70	0.074 18	—	—	5.802 12	166/3
8_{12}	0	—	—	—	—	0	176/3
8_{13}^+	0.057 06	0.715 65	0.079 35	—	—	5.905 36	56
8_{14}^+	0.099 19	0	0.099 19	—	—	5.866 47	170/3
8_{15}^+	0.055 56	0.863 05	0.068 46	—	—	4.488 64	57
8_{16}^+	0.080 02	0.199 09	0.082 08	—	—	3.091 04	58
8_{17}	0.042 71	0	0.042 71	—	—	2.944 44	58
8_{18}	0.169 17	0	0.169 17	—	—	5.213 58	191/3
8_{19}^+	0.178 11	0	0.178 11	—	—	2.447 77	42
8_{20}^+	0.112 82	0.071 41	0.113 14	—	—	7.799 55	134/3
8_{21}^+	0.049 77	0	0.049 77	—	—	2.674 15	148/3
9_1^+	0.072 19	0	0.072 19	—	—	7.430 11	57
9_2^+	0.087 63	0	0.087 63	0.890 24	0.085 75	5.662 96	170/3
9_{42}^+	0.040 13	0.466 70	0.050 49	—	—	4.043 05	157/3
9_{47}^+	0.093 75	0	0.093 75	—	—	6.565 97	63
10_1^+	0.053 63	0.238 63	0.062 86	—	—	1.791 76	64
10_2^+	0.066 35	0.895 86	0.094 63	—	—	6.013 72	200/3

J. Stat. Mech. (2012) P05003

In most cases the maximal compressibility is at zero pressure, but there are some exceptions to this in tables 9 and 10. For example, the maximum compressibility of the unknot is at $p = 0.086\,64\cdots$ for the choice $V_{\rm b}$ in table 9.

There are also some knot types with secondary local maxima in the compressibility, similar to the case seen in figure 2 for the trefoil in the SC lattice with the choice of $V_{\rm b}$ as volume. With the choice $V_{\rm b}$ in the BCC, these include 6_3, 7_1^+, 8_4^+, 8_7^+, 8_9, 8_{18}, 9_2^+ and 9_{47}^+, and for the choice $V_{\rm e}$, 6_2^+, 7_3^+ and 9_2^+.

Amongst knot types of eight crossings the knot types 8_1^+, 8_3, 8_{12}, 8_{18} and 8_{19}^+ can be realized in a rectangular box of volume 144; this is smaller than other eight crossing knots, and these knot types have compact minimal length conformations in the BCC. As one would expect, with some exceptions, these knot types are also less compressible than other eight crossing knots.

The maximum work in table 9 is obtained for 8_4^+, and $\mathcal{W}_{8_4^+} = 7.579\,68\cdots$. Other knot types which have high values for $\mathcal{W}_K$ are 8_2^+, 8_7^+ and 8_{18}.

If one considers the volume $V_{\rm e}$ instead, then there is a steady increase of $V_{\rm e}$ with increasing knot complexity in table 10. Amongst knot types of eight crossing the knot types 8_{19}^+ and 8_{20}^+ can be realized with average excluded volumes $V_{\rm e}$ equal to 42 and 134/3; this is small when compared to other eight crossing knots.

The maximum work in table 10 is obtained for 8_2^+, and $\mathcal{W}_{8_2^+} = 7.807\,92\cdots$. Other knot types which have high values for $\mathcal{W}_K$ are 8_{20}^+ and 9_1^+.

3.4. Discussion of results

The compressibility data of SC lattice knots in tables 3 and 4 indicate that different knot types may have very different properties. That is, the compressibilities are functions of the topologies of the embedded polygons, as well as of the geometries of the polygons, since the results are also dependent on the lattice, as seen, for example, when comparing the data in tables 3, 7 and 9.

Generally, the minimal length lattice knots were also more compressible in the volume $V_{\rm b}$, compared to the average excluded volume $V_{\rm e}$ which is a more close-fitting envelope about the polygon. This should be due to the fact that there is extra space for the compressed polygon to expand into near the corners of the rectangular box in the volume $V_{\rm b}$, and this is not available in the volume $V_{\rm e}$.

There appears to the little correlation between the zero pressure compressibilities of minimal lattice knots in the three lattices. For example, in figures 15 and 16 two scatter plots of the zero pressure compressibilities computed from the rectangular box volume $V_{\rm b}$ are given, showing a wide dispersion of points and little correlation between the data in different lattices. There are some generic trends visible in these plots: for example, the compressibility tends to increase with crossing number in at least one of the lattices (and knots with low crossing number are likely to be closer to the origin in these plots).

The situation is similar if the compressibilities are instead computed by considering the more close-fitting volume $V_{\rm e}$. In figure 17 a scatter plot of the zero pressure compressibilities in the SC and FCC lattices, computed from $V_{\rm e}$, is illustrated. The wide dispersion of the points is similar to the results seen for the volume $V_{\rm b}$.

Examination of the data on $\mathcal{W}_K$ in each of the lattices and for the knot types shows that there are some correlations between the compressibility and the total amount of

J. Stat. Mech. (2012) P05003

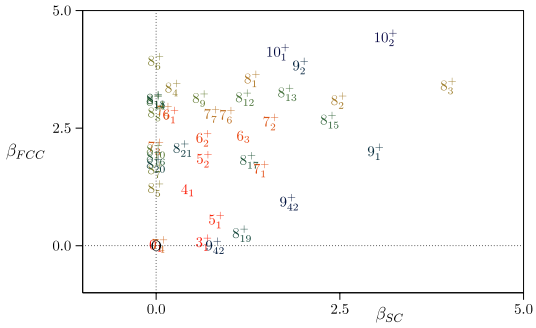

Figure 15. Scatter plot of zero pressure compressibilities (V_b) of minimal lattice knots in the SC and FCC lattices. Generally, the lattice knots are more compressible in the FCC, although there are exceptions to this, these would be the knot types which lie below the diagonal in this diagram.

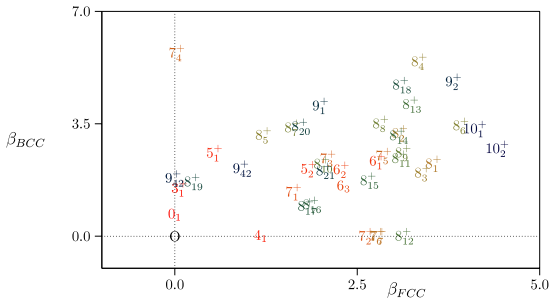

Figure 16. Scatter plot of zero pressure compressibilities (V_b) of minimal lattice knots in the FCC and BCC lattices. Generally, the lattice knots are more compressible in the FCC.

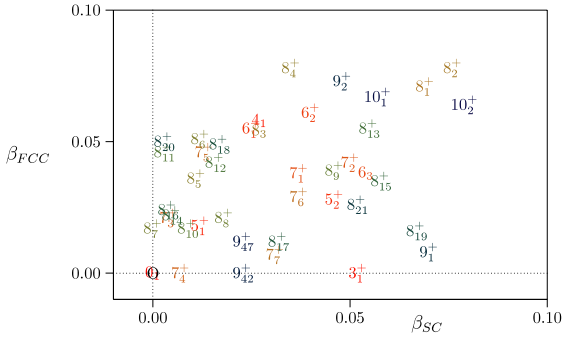

Figure 17. Scatter plot of zero pressure compressibilities of minimal lattice knots computed from the volume V_e in the FCC and BCC lattices.

work. For example, in figure 18 a strong correlation is observed between the maximum compressibility β_m and $\mathcal{W}_K$ of knot types in the SC lattice computed from the volume V_e. Similar graphs are obtained in the other lattices and also for the choice of V_b as the containing volume. There are somewhat weaker correlations between the zero pressure compressibility and $\mathcal{W}_K$ in all cases.

J. Stat. Mech. (2012) P05003

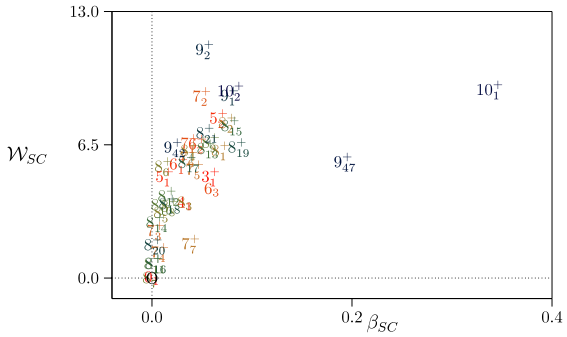

Figure 18. Scatter plot of maximum compressibilities of minimal lattice knots and the total amounts of work $\mathcal{W}_L$ computed from the volume V_e in the SC lattice. The data show a close correlation, with the knot types 9_{47}^+ and 10_1^+ clear outliers in this graph.

The data in tables 3 and 7–10 show an association between knot types having secondary local maxima in their compressibility curves, and having high total values of $\mathcal{W}_K$. In table 3 the knot types 3_1^+, 5_1^+, 6_2^+, 9_2^+ and 10_1^+ have local maxima in β_{SC} (the case for 3_1^+ is illustrated in figure 2), and all have higher values of $\mathcal{W}_K$ than comparable knots. A similar pattern can be seen in the other tables.

4. Conclusions

In this paper the compressibilities of minimal length lattice knots were examined in three lattices, namely the SC, FCC and BCC lattices. Generally, the compressibility properties were found to be dependent on the lattice as well as the knot type. Since the lattice imposes a geometric constraint on the lattice knots, the compressibility is determined to be a function of the geometry.

More generally, different knot types were also found to have very different compressibility properties in each of the lattices. This is, for example, illustrated in figures 10 and 11 for SC lattice knots; the compressibilities of knot types of roughly the same geometric and topological complexity (for example, about the same minimal length and with the same crossover numbers) are seen to be different with increasing forces.

We examined the compressibilities by using two notions of a confining space for the lattice knots, firstly the smallest rectangular box volume V_b containing the polygons, and secondly an average excluded volume V_e computed by slicing the knot into slabs, taking the convex hulls of those slabs, and then their union. V_e is a very tight envelope around the lattice knot.

In figure 6 we show that there is a strong correlation in knot type between V_b and V_e in the SC lattice, and the convex hull volume is thus similarly highly correlated with both V_b and V_e. Similar results were obtained in the FCC and BCC lattices. Thus, for many knot types the compressibilities β were similarly behaved for either choice of the volume, as one may see in figures 2 and 8 for the knot type 3_1 and in figure 9 for the knot type 4_1 in the SC lattice. This was not universally the case however, as for example seen in figure 13, where the data in the three lattices are compared for the trefoil knot.

J. Stat. Mech. (2012) P05003

Table 11. Compressibilities of compound SC lattice knots with volumes V_b (top data) and V_e (bottom data).

Knot	$\beta(0)$	p_m	max $\beta(p)$	loc p_m	loc max $\beta(p)$	$\mathcal{W}_K$	min V
$3_1^+\#3_1^+$	1.272 31	0.331 17	2.248 76	—	—	7.151 49	24
$3_1^+\#3_1^-$	1.519 49	0.204 08	1.256 17	—	—	8.425 08	24
$3_1^+\#4_1$	1.762 27	0.000 00	1.762 27	—	—	4.794 72	36
$4_1\#4_1$	2.304 17	0.032 92	2.572 05	—	—	6.770 72	45
$3_1^+\#5_1^+$	0.467 21	0.197 79	2.910 11	—	—	6.037 15	40
$3_1^+\#5_1^-$	1.504 15	0.101 67	1.733 99	—	—	7.077 41	40
$3_1^+\#5_2^+$	2.225 90	0.000 00	2.225 90	—	—	9.994 05	40
$3_1^+\#5_2^-$	0.125 13	0.247 02	0.668 74	—	—	2.908 72	48
$3_1^+\#3_1^+$	0.046 53	0.894 01	0.715 36	—	—	6.458 34	53/4
$3_1^+\#3_1^-$	0.058 39	1.280 41	0.130 51	—	—	8.425 08	97/6
$3_1^+\#4_1$	0.054 82	0.964 56	0.077 46	—	—	8.228 71	259/12
$4_1\#4_1$	0.063 22	1.428 18	0.096 18	—	—	8.850 16	51/2
$3_1^+\#5_1^+$	0.046 39	1.288 00	0.118 47	—	—	8.339 74	70/3
$3_1^+\#5_1^-$	0.045 77	1.406 75	0.101 93	—	—	9.380 00	91/4
$3_1^+\#5_2^+$	0.077 06	1.311 28	0.162 66	—	—	11.246 82	70/3
$3_1^+\#5_2^-$	0.033 21	0.954 26	0.050 34	—	—	4.007 33	101/4

We do, however, see the following qualitative features in our results. (1) The compressibilities are not monotonic with increasing pressure, but may rise and fall instead, and may even exhibit two local maxima. That is, with increasing pressure the lattice knot may become relatively more compressible in the sense that the fractional change in volume may increase with pressure in certain pressure ranges. (2) Generally, in tables 3 and 4, 7 and 8, and 9 and 10, there is a weak pattern of increasing compressibility at zero pressure down the tables. (3) We found that FCC lattice knots are likely to have larger compressibilities with the volume V_b, as seen in figures 15 and 16, although there are many exceptions to this. This is not the case if the volume V_e is used, as one may, for example, see in figure 17.

We have also computed several other properties of the lattices knots, such as, for example, the minimum values of V_b and V_e in each case. In addition, we have computed the maximum amount of useful work that can be extracted from a knot if it undergoes a reversible isothermic expansion. This sets an upper bound on the amount of useful work that can be extracted by the expansion of a compressed lattice knot. Our results were listed and discussed (see for example figure 18).

As a final set of calculations, we considered minimal length lattice knots with compound knot type in the SC lattices. Our results are listed in table 11. Note that in this short list for both choices of the volume (V_b and V_e) $3_1^+\#5_2^+$ is the most compressible and has the largest value for $\mathcal{W}_K$. Similarly, $3_1^+\#5_2^-$ is the least compressible with the lowest value of $\mathcal{W}_K$.

Acknowledgment

The authors acknowledge support in the form of NSERC grants from the Government of Canada.

References

[1] Aragão de Carvalho C and Caracciolo S, *A new Monte Carlo approach to the critical properties of self-avoiding random walks*, 1983 *Phys. Rev.* B **27** 1635
[2] Berg B and Foester D, *Random paths and random surfaces on a digital computer*, 1981 *Phys. Lett.* B **106** 323
[3] Burde G and Zieschang H, *Knots*, 1985 *De Gruyter Studies in Mathematics* vol 5 (Berlin: De Gruyter)
[4] de Gennes P G, 1979 *Scaling Concepts in Polymer Physics* (Ithaca, NY: Cornell University Press)
[5] Delbrück M, *Knotting problems in biology*, 1962 *Proc. Symp. Appl. Math.* **14** 55
[6] Diao Y, *Minimal knotted polygons on the cubic lattice*, 1993 *J. Knot Theory Ram.* **2** 413
[7] Diao Y, *The number of smallest knots on the cubic lattice*, 1994 *J. Stat. Phys.* **74** 1247
[8] Frisch H L and Wasserman E, *Chemical topology*, 1961 *J. Am. Chem. Soc.* **83** 3789
[9] Hammersley J M, *The number of polygons on a lattice*, 1961 *Math. Proc. Camb. Phil. Soc.* **57** 516
[10] Janse van Rensburg E J, 1999 *Minimal Lattice Knots* (*Series on Knots and Everything* vol 19) ed A Stasiak, V Katritch and L H Kauffman (Singapore: World Scientific) Contributed to *Ideal Knots*
[11] Janse van Rensburg E J, *Thoughts on lattice knot statistics*, 2008 *J. Math. Chem.* **45** 7 (Commemorative issue in honour of S Whittington and R Kapral)
[12] Janse van Rensburg E J and Promislow S D, *Minimal knots in the cubic lattice*, 1995 *J. Knot Theory Ram.* **4** 115
[13] Janse van Rensburg E J and Rechnitzer A, *Atmospheres of polygons and knotted polygons*, 2008 *J. Phys. A: Math. Theor.* **41** 105002
[14] Janse van Rensburg E J and Rechnitzer A, *Generalised atmospheric sampling of self-avoiding walks*, 2009 *J. Phys. A: Math. Theor.* **42** 335001
[15] Janse van Rensburg E J and Rechnitzer A, *Generalised atmospheric sampling of knotted polygons*, 2010 *J. Knot Theory Ram.* **20** 1145
[16] Janse van Rensburg E J and Rechnitzer A, *BFACF-style algorithms for polygons in the body-centered and face-centered cubic lattices*, 2011 *J. Phys. A: Math. Theor.* **44** 165001
[17] Janse van Rensburg E J and Whittington S G, *The BFACF algorithm and knotted polygons*, 1991 *J. Phys. A: Math. Gen.* **24** 5553
[18] Mann C, Mcloud-Mann J, Ranalli R and Smith N, *Minimal knotting numbers*, 2009 *J. Knot Theory Ram.* **18** 1159
[19] Michels J P J and Wiegel F W, *On the topology of a polymer ring*, 1986 *Proc. R. Soc.* A **403** 269
[20] Nishida N and Kaneko M, *The apparent compressibility of high polymers in Solution*, 1959 *J. Fac. Sci. (Hokkaido University) Japan Ser II* **5** 165
[21] Orlandini E, Tesi M C, Janse van Rensburg E J and Whittington S G, *Asymptotics of knotted lattice polygons*, 1998 *J. Phys. A: Math. Gen.* **31** 5953
[22] Pippenger N, *Knots in self-avoiding walks*, 1989 *Discrete Appl. Math.* **25** 273
[23] Portillo J, Diao Y, Scharein R, Arsuaga J and Vazquez M, *On the mean and variance of the writhe of random polygons*, 2011 *J. Phys. A: Math. Theor.* **44** 275004
[24] Rosenbluth M N and Rosenbluth A W, *Monte Carlo calculation of the average extension of molecular chains*, 1955 *J. Chem. Phys.* **23** 356
[25] Scharein R, Ishihara K, Arsuaga J, Diao Y, Shimokawa K and Vazquez M, *Bounds for minimal step number of knots in the simple cubic lattice*, 2011 *J. Phys. A: Math. Theor.* **42** 475006
[26] Sumners D W and Whittington S G, *Knots in self-avoiding walks*, 1988 *J. Phys. A: Math. Gen.* **21** 1689
[27] Vanderzande C, *On knots in a model for the adsorption of ring polymers*, 1995 *J. Phys. A: Math. Gen.* **28** 3681
[28] Zhang W and Kiran E, (p, V, T) *behaviour and miscibility of (polysulfone + THF + carbon dioxide) at high pressures*, 2003 *J. Chem. Thermodyn.* **35** 605

J. Stat. Mech. (2012) P05003